Spring 2021

Synthesis of a Series of Ag(I)-NHC Complexes for Future Antibacterial Studies

Alyssa Malto
amalto@rollins.edu

Synthesis of a Series of Ag(I)-NHC Complexes for Future Antibacterial Studies

Alyssa R. Malto

A Senior Honors Project Submitted in Partial Fulfillment of Requirements of the Honors Degree Program

May 2021

Faculty Sponsor: Dr. Laurel Goj Habgood

Rollins College
Winter Park, Florida

Table of Contents

List of Figures, Schemes, and Tables

Acknowledgments

Abstract

For thousands of years, silver (Ag) has been widely used for medicinal purposes due to its broad-spectrum antimicrobial properties. While medicinal silver usage declined with the advent of antibiotics, there has been a renewed interest in therapeutic silver coordination compounds to combat the spread of antibiotic resistance. *N*-heterocyclic carbenes (NHCs) are promising ligands for silver metallodrugs due to their wide structural variety that allows for tunability of the complex's overall steric and electronic properties and previously established bioactivity against various pathogens and cancer cell lines. There is potential for efficacy against biofilms, a type of microbial growth pattern that is common among numerous pathogens. In order to explore the impact of the steric and electronic properties of certain NHC structural features on the overall activity against *Streptococcus mutans,* the etiological agent behind cavities, a series of five Ag(I)-NHCs were synthesized over the course of three steps and characterized: [(IMes)AgCl] (**1**), [(IPr)AgCl] (**2**), [(IMes^{Me2})AgCl] (**3**), [(SIMes)AgCl] (**4**), [(IMes)AgCl] (**5**). Challenges occurred while synthesizing complex **3**, IPr·HCl (**14**), and IMes^{Me2}·HCl (**15**). Complex **1** will serve as the baseline that all other complexes will be compared to in future antibacterial studies. The diazabutadiene and imidazolium chloride precursors and Ag(I)-NHCs were synthesized with low to moderate yields. Based on the reaction mechanisms and literature protocols, increasing the amount of the catalytic reagents as well as optimization of the isolation and purification techniques should improve yields. Future work should focus on the syntheses of [(BMes)AgCl] (**6**) and [(6-Mes)AgCl] (**7**) which were unable to be completed due to time constraints. Upon successful completion of the syntheses, all will be given to the Santiago lab (Rollins Dept. of Biology) where they will be screened against *S. mutans* to assess their antibacterial activity.

Introduction

Medicinal Inorganic Chemistry: Overview & History

While the majority of compounds used medicinally are organic-based (e.g. small organic molecules, biologics), inorganic and organometallic complexes also have clinical applications. Medicinal inorganic chemistry is the study of active metal ions, coordination complexes, or salts that can be introduced into a biological system for the purposes of disease therapy or diagnosis.[1] Though metals have been used for medicinal purposes since ancient times by various civilizations, medicinal inorganic chemistry, as a formal discipline, is relatively young, having only established itself within the last century.

The foundations can, in part, be traced to back to Paul Ehrlich (1854-1915), the father of chemotherapy, who, among other accomplishments, developed salvarsan, an arsenic-based anti-syphilitic mixture, widely considered to be one of the first therapeutic metallodrugs.[1,2,3] The discovery of the anticancer activity of cisplatin (Platinol®) during the 1960s further cemented medicinal inorganic chemistry as a discipline.[1] Following this serendipitous finding, the field grew rapidly with numerous metal complexes developed for two primary purposes: disease therapy and diagnosis in the form of single-photon emission computed tomography (SPECT) positron emission tomography (PET) tracers and magnetic resonance imaging (MRI) contrast agents.[2] Therapeutic metallodrugs have been used to primarily combat ailments like rheumatoid arthritis (e.g. auranofin, Ridaura®; sodium aurothiomalate, Myocrisin®) and various cancers (e.g. carboplatin, Paraplatin®; porfimer sodium, Photofrin®). Radiopharmaceuticals such as Rb-82 chloride (Cardiogen-82®), Tc-99m bicisate (Neurolite®), and Tc-99m tilmanocept (ProstaScint®) have become diagnostic imagining mainstays.[2] Today, numerous metallodrugs have been FDA-approved with others currently in clinical trials or the earlier phases of drug discovery and development.[2]

History of Silver in Medicine

People have taken advantage of silver's antimicrobial properties for medicinal purposes since Ancient Greece. Historically, silver has primarily been used as a water purificator, a topical agent for burn and wound care, and a general anti-infective agent against various ailments.[4] The Greeks and other ancient peoples would often store water, wine, and other beverages in silver vessels to prevent spoilage; a practice that some historians theorize could have led to the adoption of silverware for eating utensils by the upper class. Later explorers and settlers during the Age of

Exploration and beyond would take advantage of this by leaving silver coins or utensils at the bottom of beverage containers.[4] Today, silver is still found in water filters with both ionic and nanosilver being investigated for both a small- and large-scale potable water disinfection.[5]

Thought to facilitate the healing process, silver was often a staple in the treatment and management of both wounds and burn injuries. Silver was primarily employed in the form of silver sutures, silver leaf and other silver-containing dressings during the 1800s.[5] In the 20th century, silver nitrate solutions were commonly prescribed for burn care. The clinical success of silver nitrate and mafenide acetate (Sulfamylon®), a sulfur-based burn treatment, led to the development of the topical burn ointment, silver sulfadiazine (Silvadene®).[6] Silver sulfadiazine and other silver-based burn and wound treatments continue to have clinical relevance to this day.

Regarding its use as a general anti-infective agent, for centuries, various silver compounds (e.g. silver salts, silver proteinates, silver arsphenamine, silver acetate) have been used to treat a wide range of maladies such as: conjunctivitis and other ophthalmic conditions, allergies, colds, gastroenteritis, gonorrhea, syphilis, mental illness, and even smoking.[4] Following the advent of antibiotics, medicinal silver use largely declined.[4] Colloidal silver, which has historically been used as a general bactericide, has largely fallen out of the medical community's favor. However, it has been coopted by those in the alternative medicine movement as a general cure-all.[4] The rise of antibiotic and multidrug resistance in bacteria within the last few decades has led to a renewed interest in silver as a potential alternative.[7] In particular, silver (Ag) has shown promise as a potential therapeutic agent due to its broad-spectrum antimicrobial properties.[4]

Chemical Properties and Biological Activity of Silver

Chemical Properties, Bioavailability, and Toxicity

Silver is a lustrous pale grey noble metal that can form three bioactive oxidation states (Ag^+, Ag^{2+}, and Ag^{3+}) each capable of forming coordination complexes.[8,9] While many metals play an integral role in many biological processes and biochemical pathways, noble metals like silver are not considered essential for life. However, their resistance to oxidation and corrosion makes them useful for a variety of purposes, including biomedical applications.[10,11]

Silver can enter the body via absorption, ingestion, and inhalation followed by cellular uptake. The exact mechanism varies by cell type. Entry of silver into the human body usually occurs via trace contamination in food and water supplies or occupational exposure.[4] While the majority of ingested silver is ultimately excreted out of the body via feces, as much as 10% is still

absorbed.[4] Though solid silver is insoluble in aqueous solutions, ionization in the presence of an oxidant can release reactive silver cations. What happens to silver in the body is dependent on the mode of entry and the form it is in (i.e. solid, ionic, or nano) as different biological anions (e.g. chloride, nitrate, sulfate, acetate, oxalate), biomolecules (e.g. proteins, nucleic acids), and environments (e.g. pH, exposure to sunlight) can impact cationic silver's solubility, thus reducing the amount of the bioreactive species.[4]

All toxicities are dose-dependent: too low of a concentration will result in little or no effect, too high will lead to toxicity, with the optimum physiological response range lying between the two.[13,14] Silver is especially toxic to lower organisms, termed the oligodynamic effect, killing bacteria and other microbes at very low concentrations.[6] Additional studies have also shown that silver possesses cytotoxic properties.[4] While cell destruction is harmful and can result in tissue and organ damage, there are times when this is advantageous. Silver's cytotoxicity can be modulated via host-guest chemistry or other methods to kill cancerous cells or microbes while sparing healthy cells opening the doors to potential clinical applications.[15,16]

Overall, silver is primarily non-toxic to humans. While humans can tolerate low doses of silver, repeated exposure over time can result in negative effects such as silver accumulation in tissues, particularly those of the reticuloendothelial organs.[4,17] The most well-known side effect of silver overload in humans is argyria, a permanent skin discoloration that can be attributed to sunlight-induced reduction of ionic silver in the skin. The resulting nanoparticles can form insoluble sulfides and selenides, causing the skin to turn blue-grey. Argyria can be localized to one or more specific areas or spread all over due to the transport and deposition of silver throughout the body via the bloodstream.[4] As the majority of cases of argyria are due to excessive long-term exposure, this should not discount the establishded benefit and further potential of silver in the clinic. If silver is to continue to play a role in the future of medicine, research must continue behind the mechanisms behind silver's absorption, distribution, metabolism, and excretion (ADME) and toxicity in order to effectively and safely administer and deliver silver-based therapeutics.

Silver's Mechanism of Action

The mechanism behind silver's cytotoxic activity is multifaceted, dependent on cationic silver's interactions with biomolecules and other cellular components. Positively charged Ag ions can react with both electron-rich functional groups (e.g. nitrogen, sulfur, and oxygen-containing moieties) and anions (e.g. PO_4^{3-}, Cl^-, carboxylates) within cells and the bloodstream to form stable

complexes, altering the shape and charge of the overall compound and impairing a biomolecule's function.[2,3,7] Occasionally, the bonds holding these Ag-biomolecule complexes together can break, generating silver-free radicals that cause intracellular damage that is compounded by the suppression of oxidative stress responses.[8,18] Studies on *Escherichia coli* have shown that Ag cations inhibit the energy-producing reactions of cellular respiration by damaging enzymes involved in glycolysis and the citric acid cycle.[16] Furthermore, they disrupt iron-sulfur clusters which play a key role in electron transfer during the final stage of cellular respiration.[4] Silver cations can also damage cell membrane integrity and inhibit cell replication by chelating to embedded proteins and nucleotide bases, respectively, as well as impair ion and nutrient concentration gradients and exchange.[4,8] In bacteria specifically, electrostatic interactions between silver cations and the anionic portions of the cell membrane have been shown to inhibit bacterial movement or rupture the membrane, resulting in the release of key metabolites and amino acids.[8] Furthermore, silver has been shown to trigger a stress response in bacteria, inhibiting growth, division, and metabolism, rendering them viable, but not culturable (VBNC).[19] When a bacterium finally does succumb to silver, it can serve as a reservoir for Ag ions that, when released, kill more bacteria, resulting in a so-called "zombie" effect.[20] Given the numerous mechanistic effects that need to be overcome, silver resistance is rare in nature. While some silver-resistance genes do exist, studies have found that bacterial silver resistance can be overcome with sufficiently high concentrations of silver.[8]

Current and Developing Applications of Medicinal Silver

Outside of the realm of wound and burn care, silver-treated or -coated indwelling medical devices, such as central venous lines, Foley catheters, and endotracheal tubes, have become popular due to their ability to prevent hospital-acquired infections (HAIs) and biofilm development.[6] With regards to the future of medicinal silver, several different forms of silver are currently being explored by those developing novel therapeutics (**Figure 1**).[4,7] For example, several studies involving silver clusters have shown their potential for a wide range of biomedical purposes from theranostics to drug delivery.[21,22] A similar class of compounds, the silver metal organic frameworks (MOFs), have also been explored as potential antibacterial agents. Studies have indicated that AgMOFs behave similarly to the aforementioned "zombie" bacteria, acting as a silver reservoir resulting in sustained released of Ag ions over time.[23]
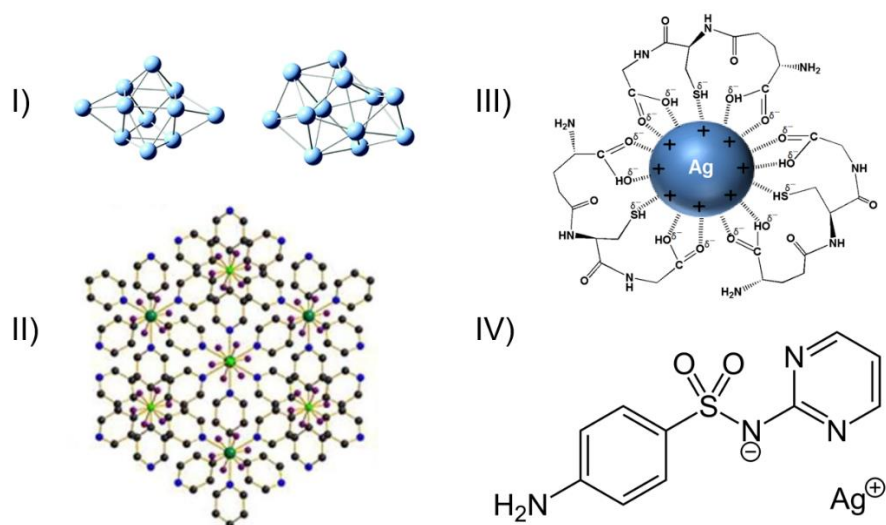
Figure 1. Classes of silver-based medicinal agents. I) Clusters. II) Metal organic frameworks. III) Nanoparticles. IV). Coordination complexes. Structures and figures adapted from *RSC Advances*. Royal Society of Chemistry. January 18, 2019, 2673–2702.; *Phys. Chem. Chem. Phys.* **2017**, *19* (29), 19360–19368.; *Inorg. Chem. Commun.* **2020**, *112*, 107733.; and Wikimedia Commons.[24-27]

Much attention has been given to silver nanoparticles which have shown to be effective against a wide variety of pathogens and cancer cell lines. The use of AgNPs in medicine is not a new idea as colloidal silver is an aqueous suspension of nanosilver.[4] Silver nanoparticles' diversity in structure and composition make them suitable for a wide range of biomedical purposes, from theranostics to incorporation into biomaterials. According to the NIH, there are currently 28 clinical trials that involve AgNPs.[28] Of those 28, only 14 have been completed. The remainder are either still recruiting or not yet recruiting or have been withdrawn, terminated, or an unknown status. Four have either completed or are currently in Phase 4 clinical trials, meaning the AgNPs in question have already been FDA approved and are being studied to gain further insight into their safety safety, efficacy, or optimal use.[29] These studies included: a central venous catheter that was impregnated with AgNPs (AgTive®), AgNP-containing skin wipes (Theraworx) and a bioceramic sealer, and a nanosilver combined CaOH intracanal medication to treat post-operative pain following failed root canals.[30-33] Likewise, the majority of the trials listed involved either AgNPs incorporated into existing medical treatments, devices, or tools for oral/dental applications. More research needs to be done as studies have shown silver nanoparticle can accumulate within tissues and are toxic to various human cell lines.[4] Currently, there have been two clinical trials assessing

the AgNP toxicity in humans in Phase 1 and Phases 1 and 2, respectively, that were both conducted by Munger and coworkers.[34-36] After orally dosing study participants with AgNPs, various body samples and measurements were taken. Researchers did not find any clinically important changes in metabolic, hematologic, or urinalysis measurements, pulmonary reactive oxygen species and pro-inflammatory cytokine levels, or morphological changes in the lungs, heart or abdominal organs.[36] While this is very promising, it was noted that more studies involving increased dosage and exposure length and other organ systems are needed to fully determine the toxicity threshold in humans.[36]

Another promising alternative is silver-based metallodrugs or silver coordination complexes. As the case of cisplatin shows, the therapeutic potential of metallodrugs cannot be understated. While silver coordination complexes are commonly evaluated for their catalytic properties, more researchers have begun to recognize the untapped therapeutic potential and assess their bioactivity.[17] Numerous silver complexes bearing various ligands have been screened against a wide variety of microbes (i.e. Gram-positive, Gram-negative, and antibiotic-resistant bacteria, fungi, and parasites) and have shown promising results.[17] As will be elaborated on in the next section, the ligands coordinated to the central silver ion heavily influence the shape and properties of the overall complex.

Metallodrugs and Rational Drug Design

As previously mentioned, silver has three oxidation states: Ag^+, Ag^{2+}, and Ag^{3+}; all of which can form coordination complexes.[8,9] While silver(II) and silver(III) complexes display higher reactivity, they have the drawback of being less stable, and therefore less effective, while *in-vivo* due to their higher oxidation states.[4,9] Regardless, the reactive part of all silver metallodrugs is the coordinated silver ion.[4] As previously noted, silver ions can complex with many common biological functional groups. For a silver complex to be an effective drug, it needs to be more discriminative, targeting a specific site on protein or a specific DNA sequence.

Rational drug design, or structure-based design, can trace its roots to Paul Ehrlich's *Zauberkugel Theorie* or magic bullet concept. *Zauberkugels* are hypothetical agents that can effectively kill an invading pathogen without harming the body itself.[3] According to rational drug design, structural data from a specific biomolecular target and/or biochemical ligand should be used to design and optimize potential lead compounds.[37] Ideally, the lead should be as complementary as possible to the targeted binding site in both shape and charge to minimize off-

target effects.[2] Regarding silver metallodrugs, modularity in design allows for variability in both the type and number of ligands surrounding the central metal ion, resulting in numerous possible three-dimensional structures and electronic distributions that can be customized to each target binding site.[2] Nevertheless, even if a drug was rationally designed, there is no way to predict precisely how the drug will react *in-vivo*.

For metallodrugs specifically, a key concern is the possibility of ligand exchange or transmetalation with antitargets which, in the case of silver complexes, can cause premature silver ion release. However, these processes are less likely to occur if the silver complex is sufficiently stable. Specifically, the overall silver coordination complex must have a relatively high stability constant (β) to remain intact as it travels throughout the bloodstream to the intended target and interacts with various ligands. As such, the silver-ligand bonds within the complex must be sufficiently strong.[2] Regarding metallodrugs, the steric and electronic properties of the ligand(s) coordinated to the central metal have a significant influence on the physiochemical properties of the metallodrug, dictating its pharmacokinetics and overall efficacy.[2] While various types of ligands have been coordinated to silver, phosphines, those bearing nitrogenous heterocycles (e.g. phenanthrolines, pyridines, polypyridines), and current drug molecules (e.g. Metronidazole, Carbocysteine; coumarins) are the ligands that have shown the most promising results.[4,17]

Currently, the Habgood lab, in conjunction with the Santiago lab (Rollins College Dept. of Biology), is exploring the efficacy of various silver compounds against *Streptococcus mutans*. As of now, six silver(I) salts bearing various cyanoximate ligands have been synthesized by the Habgood lab. The cyanoxime ligand family, characterized by C=NOH moieties, include both a cyano group (C≡N) and a variable R group bonded the imine carbon (**Figure 2**).[38]
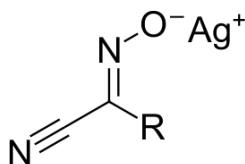
Figure 2. A generic silver(I) cyanoximate complex.

The Santiago lab has started to screen these compounds against *S. mutans*, producing promising results. However, more research needs to be done on the stability of Ag(I) cyanoximates while in solution and the reactivity of the cyanoximate anion itself, especially since it bears a cyano group.[39] There is the possibility that the cyano group could break off while *in-vivo* and cause

cyanide poisoning which would be problematic. Given their established biofilm activity, high stability, and steric and electronic tunability, silver(I) *N*-heterocyclic carbenes (NHCs), or Ag(I)-NHCs, have the potential to be more effective against *S. mutans*. A previous study screened several pyrazine-functionalized Ag(I)-NHCs against *S. mutans* and found that their minimum inhibitory concentration (MIC) values ranged between 4-32 μg/mL (**Figure 3**).[40]
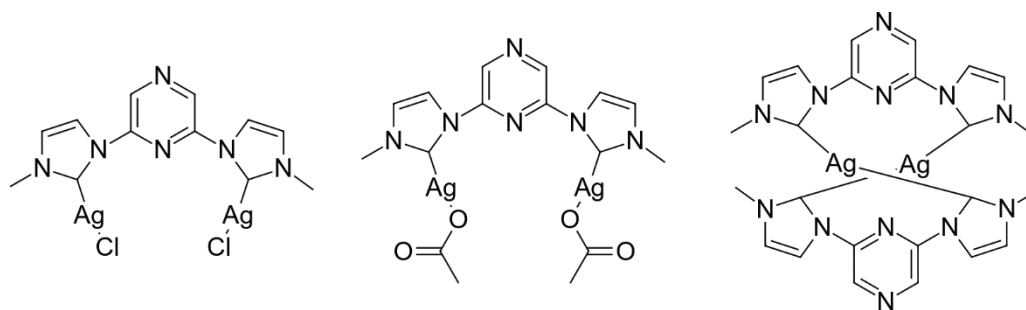
Figure 3. Pyrazine-functionalized Ag(I)-NHCs previously screened against *S. mutans*. Adapted from *Curr. Med. Chem.* **2012**, *19* (24), 4184–4193.[40]

N-Heterocyclic Carbenes

Structural and Electronic Properties

Of the previously mentioned ligand families, *N*-heterocyclic carbenes (NHCs) are some of the most attractive. For a ligand to be an NHC, it needs to be a heterocycle (a ring system composed of at least two different elements) that contains a carbene carbon (a neutral, divalent carbon atom with two unshared valence electrons) and at least one nitrogen (**Figure 4**).[41] General NHC structural features include: the nitrogen heteroatom(s) with bulky substituent(s) bonded to the nitrogen atoms and the size and composition of the ring backbone. The steric and electronic effects of these features help stabilize the carbene carbon and make it nucleophilic, allowing it to coordinate to transition metals, like silver, and form stable complexes.
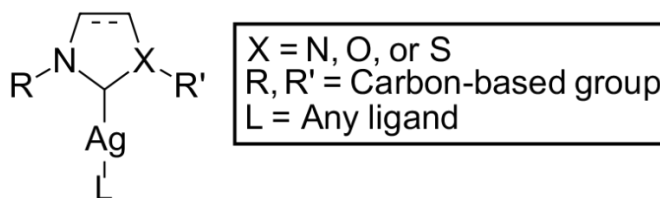
Figure 4. A generic silver-NHC complex. R and R' may be identical or different, vary in size, and/or possess electron-donating or withdrawing groups.

In general, NHCs are classified as L-type ligands, meaning they are neutral Lewis bases that donate two electrons during the formation a coordinate covalent bond.[42] They are considered strong σ-donor ligands, due to the high energy level of the highest occupied molecular orbital (HOMO).[43] While there are several different methods to experimentally evaluate a given NHC's donor-acceptor properties, the electronic variation between individual NHC ligands can be ascribed to differences in the backbones and R substituents. There are two main factors: the inductive effect (I) and the mesomeric or resonance effect (M/R). The inductive effect deals with the presence of electron-withdrawing (-I) or electron-releasing groups (+I), while the mesomeric effect is concerned with lone pair donating (+M) and withdrawing (-M) ability. The inductive and mesomeric properties of a given heteroatom or functional group can either increase the overall NHC electron density, improving its donor ability, or decrease it and make it a poor donor.[43]

N-Heterocyclic Carbenes versus Phosphines

Phosphines are another family of L-type ligands comprised of organophosphorus-based compounds. Their denticity can vary, with mono-, bi-, tri-, and tetradentate phosphines both commercially and synthetically available. The symmetry or lack thereof between the R groups attached to the phosphine atom can be used to broadly classify phosphines into three main classes: homoleptic (PR_3), heteroleptic (R_2PR'), and asymmetric or P-chiral phosphines ($PRR'R''$) (**Figure 5**).[44] The identity of said R groups can be used to modulate both the steric and electronic properties of the overall complex.[44] Of the three classes, heteroleptic phosphines are the easiest to synthesize and tailor, opening the doors to a wide variety of purposes. Since their widespread adoption in during the mid to late 20th century, phosphines have established themselves as an important class of ligands when designing and synthesizing transition metal complexes, especially within the field of catalysis.
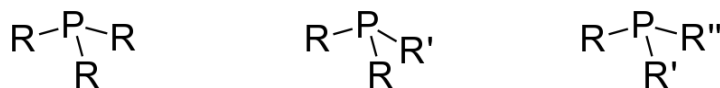
Figure 5. Classes of phosphines. I) Homoleptic. II) Heteroleptic. III) Asymmetric. R, R', and R''' can be Hs, alkyls, aryls, or other organic groups.

Other applications beyond catalysis include inorganic/organometallic synthesis as well as materials, solid state, and medicinal chemistry.[44] Indeed, silver phosphine complexes have been

explored as both potential antibacterial and anticancer agents, exhibiting activity against strains of *E. coli, Salmonella typhimurium,* and *Staphylococcus aureus* as well as various cancer cell lines.[17] Their anticancer activity can be attributed to both their interactions with DNA, with some derivatives exhibiting intercalation, and their lipophilicity. However, such a high lipophilicity presents aqueous solubility issues, making them unsuitable for environments like the bloodstream and mouth, thus necessitating the presence of more polar co-ligands to expand their usage beyond topical agents like ointments and creams.[17]

Compared to Ag-phosphines, Ag(I)-NHCs do not have those solubility issues with some Ag(I)-NHC complexes remaining stable in aqueous solution for up to 17 weeks due to the presence of electron-withdrawing groups on the central imidazole.[17] Other studies have shown that NHC coordination compounds have higher thermal and oxidative stability than similar phosphine complexes making them more suitable for medicinal applications.[41] This is because the high stability of Ag(I)-NHCs allows for sustained release of silver over time, which can be beneficial for both cancer treatment, stopping bacterial infections, and preventing reinfection from occurring.[17] Furthermore, NHC-transition metal bonds are less prone to dissociation than phosphine-transition metal bonds. This makes Ag(I)-NHC complexes more likely to withstand travel through the bloodstream and arrive at their target without premature silver release, thus minimizing off-target effects.[17,35]

The higher stability of Ag(I)-NHCs can be attributed to the electronic differences between these two families of ligands. While both are L-type ligands which donate a lone pair, phosphines possess a non-directional s-type lone pair whereas NHCs have highly directional sp^2-type lone pairs, making NHCs stronger σ-donors.[45] Additionally, while both ligands are σ-donors, phosphines are also π-acceptors allowing for π-backbonding interactions. As a result, metal-NHC bonds are more electron-rich than similar metal-phosphine bonds, making the metal-carbene carbon bond the stronger of the two.[45] Regarding synthetic tractability, when the first NHC synthesis was reported by the Arduengo group, NHCs were largely considered to be less convenient phosphine alternatives as they were not commercially available and difficult to synthesize. Following the discovery of the catalytic activity of NHC-transition metal complexes, NHCs have become more widely adopted with numerous synthetic routes published and optimized, making these ligands relatively straightforward to synthesize if they are not commercially available.[46] All of these factors combined with the structural versatility that allows

16

one to tailor both the sterics and electronics make NHCs good ligands for silver-based metallodrugs.

Silver(I) *N*-Heterocyclic Carbene Complexes: Ag(I)-NHCs

Bioactivity of Ag(I)-NHCs

Numerous studies have been conducted on silver-NHC complexes, evaluating both their anticancer and antimicrobial properties. Although cisplatin and other platinum(II)-based metallodrugs have been traditionally used as chemotherapeutics, the numerous adverse effects associated with platinum(II) drugs as well as both inherent and acquired platinum resistance has generated a pressing need for less toxic and more effective anticancer agents.[47,48] Various Ag(I)-NHCs have been tested against a wide range cancer cell lines, such as OVCAR-3 (ovarian), HCT8 (colon), UKF-NB-3 (neuroblastoma), A549 and A549R (normal and cisplatin-resistant lung), and more.[49] While cytotoxicity varies and is dependent on both the complex structure as well as the cancer cell line, in general, Ag(I)-NHCs display comparable or improved activity compared with cisplatin and other standard anticancer chemotherapeutics. Overall, Ag(I)-NHCs have been found, among other things, to inhibit cancer cell growth, restore apoptosis, and decrease tumor mass with low cytotoxicity toward noncancerous cells.[4,49,50]

Regarding Ag(I)-NHCs' antibacterial activity, numerous studies have shown effectiveness against both Gram-positive and Gram-negative bacteria.[49] Even more promising is their activity against antibiotic resistant strains of *S. aureus*, *Pseudomonas aeruginosa,* and *Burkholderia cepacia*.[49] Furthermore, Ag(I)-NHCs, especially ones possessing aromatic NHCs, are active against biofilms, which are inherently antimicrobial-resistant.[4,51] Biofilms are a growth pattern in which bacteria or other microbes aggregate together and generate an extracellular polymeric substance matrix that acts as a protective barrier.[51]

Biomedical Applications of Ag(I)-NHCs

Biofilms are especially problematic since they grow on a variety of surfaces including those of medical devices. The majority of nosocomial infections are due to biofilm growth on an implanted medical device.[52] This often results in device failure and necessitates its removal to treat the subsequent infection. To combat this potentially deadly problem, various antimicrobial coatings (AMCs) have been developed to prevent biofilm growth. AMCs fall under two categories: antibiotic-eluting device coatings and non-drug eluting coatings, which include metallic (e.g.

silver-based) coatings.[53] Due to their antibiofilm activity, Ag(I)-NHCs could potentially be incorporated within AMCs, possibly acting as a hybrid of the two main types.

Not even our own mouths are spared from biofilm intrusion. Over hundreds of different species of bacteria reside within the oral cavity. Dental plaque occurs when these metabolically active microbes colonize and anchor on to the surfaces of our teeth.[54] Bacterial metabolism results in several changes to the surrounding environment, resulting in the degradation of the outer layers of dental tissue which, if left untreated, results in cavities. The main culprit behind dental caries is the Gram-positive bacterium, *Streptococcus mutans*. The etiology of dental caries can be attributed to *S. mutans* irreversibly binding to teeth and producing high concentrations of glucans (a polysaccharide) and lactic acid, resulting in the dissolution of the hydroxyapatite crystals $[Ca_5(PO_4)_3(OH)]$ that strengthen enamel and dentin.[54] Given the high incidence and widespread distribution of dental caries, there is a vested interest in finding ways to combat *S. mutans*.

Specific Aims

Overview

In order to determine how ligand sterics and electronics affect the strength of the Ag-C bond and the overall antibacterial activity of the complex, a series of seven Ag(I)-NHC complexes coordinated to different NHCs were originally selected to synthesize with the complex, [IMesAgCl], (**1**) acting as the baseline against which all other complexes will be compared. Of the seven proposed compounds, only five were successfully synthesized (**Figure 6**).
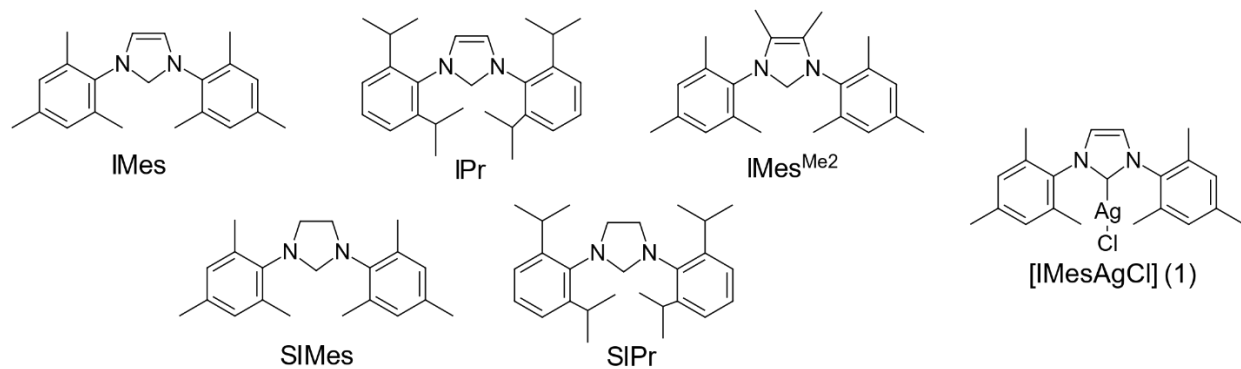
Figure 6. Target ligands and baseline Ag(I)-NHC complex, **1**.

While all the ligands have different electronic environments, the primary electronic factor chosen for investigation was the impact the of the backbone double bond. Of the five synthesized compounds, three were coordinated to ligands (IMes, IPr, and IMes^{Me2}) that possessed at least one

pair of pi backbone electrons, while the remainder (SIMes and SIPr) had saturated heterocycles. The distinguishing factor between electronically similar ligands are the steric properties. Ligands differ due to alterations to the nitrogenous substituents as is the case for IMes and IPr and SIMes and SIPr. For those ligands, the nitrogens can either be attached to mesitylene groups or more sterically hindered diisopropylphenyls. The remaining NHC, IMes^{Me2}, has increased steric bulk due to the addition of methyls directly to the backbone.

Outline of Experimental Work

The complexes, [Ag(IMes)Cl] (**1**), [Ag(IPr)Cl] (**2**), [Ag(IMes^{Me2})Cl] (**3**), are to be synthesized over the course of a three-step synthetic route based on the literature (**Scheme 1**).[46, 55-60] Diazabutadiene precursors (**8-10**) are first prepared via a condensation reaction wherein arylamines undergo a condensation reaction with either glyoxal or diacetyl. After which, an electrocyclization reaction would be used to generate imidazolium chlorides (**13-15**).[46,55,56,58,59] The imidazolium salts are then coordinated to silver using Lin's method to generate **1-3**.[57] Complexes, [Ag(SIMes)Cl] (**4**) and [Ag(SIPr)Cl] (**5**), will bypass the first two steps of that reaction pathway by coordinating commercially-available salts, **16** and **17**, to the silver.[60] Following the completion of the syntheses of the target molecules, both the Ag(I)-NHC complexes and NHC salts will be given to the Santiago lab to be screened against *S. mutans*. The results generated from the Santiago lab will inform the choice of structural features for the next series of compounds.

Results and Discussion

Target complexes **1-5** and their precursors (**8-10**, **13-15**) were successfully synthesized using published procedures with low to moderate yields (**Scheme 1**). [55-60] Compounds were characterized via ^{1}H NMR and spectra were compared to previously reported NMR data to confirm identity. [55-62]
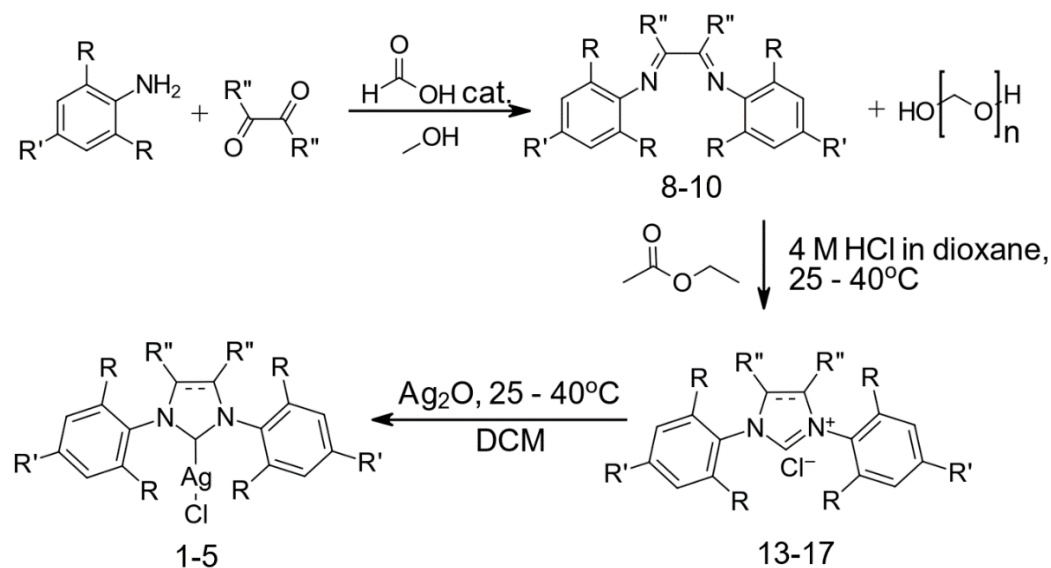
Scheme 1. Synthesis of **1-5**, **8-10**, and **13-15**. [55-60]

Syntheses of Diazabutadienes

Compounds **8-10** were all synthesized using the same method: two arylamines (i.e. 2,4,6-trimethylaniline or 2,6-diisopropylaniline) undergo successive condensations reactions with a dicarbonyl compound (i.e. glyoxal or 2,3-butanedione) to generate the corresponding diimine or diazabutadiene. [46] All three diazabutadienes were successfully synthesized with moderate yields that were lower than the reported yields: 71% (Lit.= 85-95%), 64% (Lit.=80-90%), and 57% (Lit. = 68%) for **8**, **9**, and **10**, respectively. [55,58] This could be due to the fact that the condensation reaction is reversible and that the reverse reaction, imine hydrolysis, could be occurring, thus regenerating the starting material and resulting in lower yields. [46] Because this reaction is acid-catalyzed, having an insufficient amount of catalyst present within the system could limit the amount of product generated within a given period the catalyst may get saturated, thus forcing some reactants to undergo condensation at the slower, uncatalyzed rate. Finally, excessive washing of the isolated product could result in loss of yield.

20

Syntheses of Imidazolium Chlorides

Of the three imidazolium salts that were synthesized, IPr·HCl (**14**) and IMes[Me2]·HCl (**15**) required multiple attempts. The first attempt at synthesizing **14** involved a procedure from the Nolan group.[55] However, the resulting ^{1}H NMR data differed from their reported results, indicating **14** was not successfully synthesized. Another attempt was made using the same protocol that was adapted to have a longer heating time (65 hr vs the original 1 hr) at a lower temperature. However, the reaction dried out and attempts to salvage the reaction through the addition of more solvent failed.

Further research revealed additional methods to synthesize **14** from the Jones group and Lamaty, Bantreil, Métro and coworkers.[56,58] The reaction conditions reported by Lamaty and coworkers differed significantly from the previous attempts: the solvent was changed from ethyl acetate to THF and the reaction mixture was heated at a lower temperature over the course of several days.[55,58] After heating the solution for six days, no color change had occurred and the resulting work-up yielded almost no product. No attempts at characterization were made since as there was insufficient material to prepare an ^{1}H NMR sample. Compared to the Nolan protocol, the Jones procedure did not require heat and had additional steps for the work-up beyond washing with ethyl acetate.[55,56] ^{1}H NMR spectra analysis indicated **14** was successfully made using the Jones protocol with a moderate yield (53%). Later examination of the ^{1}H NMR data from the first attempt at synthesizing **14** found that, while the data did not match what the Nolan group reported, they did match the peaks reported by the Jones group.[55,56] Further analysis is required to determine the identity of the sample as there are two impurities at 4.70 ppm (s, 1H) and 3.69 ppm (s, 1H) that cannot be accounted for. If the impurities were not part of the reaction solvent, it may still be possible to eliminate them using the Jones work-up.[56]

Likewise, imidazolium chloride **15** required multiple attempts to synthesize. Originally, **15** was to be synthesized using a protocol from the Lamaty group. However, given the significantly low yields that occurred while using their protocol to make **14,** a protocol from the Louie laboratory was used instead.[58,59] Difficulties were encountered during the isolation process following the bicarbonate wash since concentrating the reaction mixture *in vacuo* generated an oily residue. However, trituration with pentane afforded crude **15** with a low yield (34%). Attempts at obtaining pure **15** via recrystallization failed. Slow diffusion failed to produce any solid while standard multi-solvent recrystallization generated a white powder. However, the absence of all

reported ^{1}H NMR peaks indicated it was not **15**.[59] A different purification protocol for **14** from the Lamaty group was found to eliminate the color from the crude **15**, generating a white powder.[58] However, analysis did not indicate any significant difference between the ^{1}H NMR spectra of the crude **15** pre- and post-work up.

A second batch of **15** was made following failed attempts to synthesize complex **3** using crude **15**. For this reaction, a new bottle of 4 M HCl in dioxane was used. Compared to the first attempt, this reaction's progression appeared more promising since, after the addition of the paraformaldehyde-HCl solution, the solution turned the desired color (red), and not blood orange like the first attempt.[59] Unlike the first attempt, the resulting precipitate from that reaction was terracotta brown rather than light brown. Greater care was taken during the second attempt to ensure that the precipitate was as clean as possible prior to the bicarbonate wash to avoid the purification issues from the last attempt. Approximately 2.5 L of diethyl ether was initially used to wash the compound. However, visual inspection of the filtrate indicated that the precipitate was not fully clean. As such, the precipitate was stored in 100 mL diethyl ether and allowed to stir for 18 days. The long wash time had some impact as the isolated solid became light brown. During this attempt, trituration with pentane yielded both brown granules and a brown solid. However, NMR analysis indicated that the granules were impurities and were thus discarded. Using the Lamaty purification protocol again was found to successfully afford pure **15** with a 16% yield.[58]

The differences in appearances observed between the first and second attempts at synthesizing **15** suggest that the 4 M HCl in dioxane originally used during the first attempt at **15** might not have been the correct molarity due to its age as the bottle was obtained in June of 2017. This is further supported by the increased yield during later attempts at synthesizing **13** and **14.** Prior to the change in the reagent, the highest yield obtained for **13** was 37% and 53% for **14**. After switching, yields increased to 90% and 70% for **13** and **14**, respectively. During these later attempts, the paraformaldehyde-HCl solutions were observed to have a different appearance. The solutions appeared pale amber compared to the cloudy white solutions with visible particles of undissolved paraformaldehyde from the first attempts.

The discrepancies in visual appearance and yields between the early and later attempts can be explained by the reaction mechanism. All imidazolium chloride salts were synthesized from the diazabutadiene precursors by way of a sigmatropic reaction in which paraformaldehyde was introduced as the C_1 precarbenic unit (**Scheme 2**).[46] Prior to its addition to the diazabutadiene

solution, the paraformaldehyde must be dissolved in 4 M HCl in dioxane. This not only provides a source for the chloride counterions, but it allows for the *in-situ* generation of formaldehyde. Once the two solutions are combined, the formaldehyde is susceptible to nucleophilic attack from the diazabutadiene, resulting in a 1,5-dipolar cyclization at the end of which forms an imidazole wherein the formaldehyde carbon is now the carbene carbon.[46]
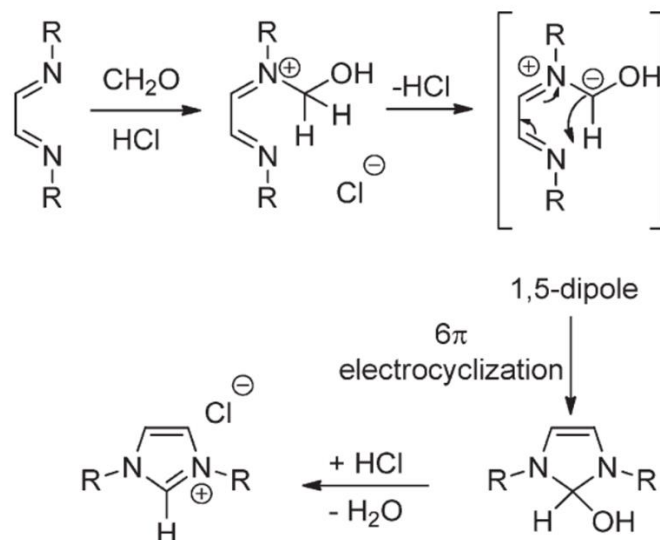
Scheme 2. Imidazolium chloride formation mechanism. Formaldehyde is generated *in situ* via the depolymerization of paraformaldehyde in an earlier step. Scheme adapted from César et al. *Chem. Rev.* April 13, 2011, 2705–2733.[46]

Previous literature has shown that in aqueous solution, the depolymerization of paraformaldehyde can be catalyzed by the presence of a base, an acid, or heat.[63] Since the depolymerization reaction is endothermic, the addition of heat can often increase the rate with organic solvents, like dioxane, acting as a heat transfer media.[64] During the first attempts at synthesizing **13-15**, it is likely that there was insufficient HCl available to catalyze the depolymerization of paraformaldehyde due to the decrease in the reagent's concentration overtime. As a result, the maximal yields for those reactions were greatly restricted, dependent upon the amount of formaldehyde was generated *in situ* rather than the amount of diazabutadiene.

Syntheses of Ag(I)-NHCs

The only silver-NHC complex that required multiple attempts to synthesize was [(IMesMe2)AgCl] (**3**). A review of the literature found only one reported synthesis of **3** by Lamaty and coworkers.[58] However, their protocol involved non-standard synthetic techniques and relied upon the use of

mechanochemical methods (i.e. vibratory ball-milling). Because of this, the synthetic protocols for **1**, **2**, **4**, **5** were used as guidance to design the synthesis of **3**.[58,60] At the time, attempts at purifying the complex's corresponding salt, **15**, had failed so crude **15** was used in the synthesis of complex **3**, under the assumption that the impurities present could be separated during the recrystallization process. For the crude complexation reaction, the reaction mixture stirred at RT for 24 hr under nitrogen. Following this, half of the solution was taken out of the glovebox, while the remaining half remained under nitrogen and was refluxed for a total of 12 hr. Both solutions were isolated using the same methods as **1**, **2**, **4**, **5** and were recrystallized with pentane at 0°C.[58.60] After a week, the black solutions and the black flakes that recrystallized out were characterized via ^{1}H NMR. Spectra analysis indicated no significant difference between the refluxed and non-refluxed samples. The ^{1}H NMR spectra of both solids indicated incomplete complexation, as both peaks from the starting material and the reported peaks of **3** were present and overlapping.[58]

Based on those results, ^{1}H NMR was used to monitor the complexation of **15** to silver in dichloromethane-d_2 during the next attempt at synthesizing **3** (**A1**). For the complexation study, purified **15** was able to be used. The resulting ^{1}H NMR indicated that after 14 hrs peaks at 9.86, 7.13, 2.39, 2.10, 2.06, and 1.74 ppm disappeared (**A1**). Based on the reported ^{1}H NMR peaks of **3** and **15**, the peaks at 7.13, 2.39, 2.10, 2.06, and 1.74 ppm likely do not correspond to the reactants or products and indicate impurities present within the initial reaction mixture.[58] However, the disappearance of a miniscule peak at approximately 9.86 ppm suggests that the carbene H is no longer present, indicating that complexation did occur.[58] However, ^{1}H NMR analysis indicated that both **3** and **15** were likely still both present within the reaction mixture. Because of the identical splitting patterns and integrations as well as the closeness of the reported chemical shifts of **3** and **15**, it was difficult to conclusively determine if the complexation was successful.[58] As a result, the complexation reaction was scaled up to obtain a more definitive result. For that reaction, pure **15** and Ag_2O were dissolved in DCM and the reaction mixture was heated to approximately 40°C and allowed to stir at 94.5 hr followed by a 70.5 hr RT stir. Again, the solution was isolated using the same methods as **1**, **2**, **4**, **5** and recrystallized from DCM with pentane at 0°C. NMR analysis indicated that complex **3** was successfully synthesized with a percent yield of 46%. While this protocol resulted in a lower yield than Lamaty and coworkers (Lit. = 81%), it bypasses the need for a stainless-steel vibratory ball mill.[58]

24

Complexes **4** and **5** were successfully synthesized with yields that were consistent with those reported in the literature: 77% (Lit.= 71%) and 63% (Lit.= 74%) for **4** and **5** respectively.[60] Complexes **1** and **2** were successfully synthesized with yields of 43% and 22%, respectively, using a protocol from the Vasam group.[57] Unfortunately, they did not report their yields for **1** and **2**. However, a search of the literature found that reactions with using the same reagents reported yields of 62% and 88% for **1** and **2**, respectively.[60,61] Discrepancies between yields could be explained by examining both the reaction mechanism and the protocol conditions.

All five complexes were synthesized via Lin's method, which is the most common method of synthesizing Ag(I)-NHCs since the reaction can be easily monitored, tolerates oxygen and a wide variety of solvents and solvent mixtures, and does not require solvent pretreatments or additional base.[65,66] Lin's method is dependent on the deprotonation of the NHC by the silver base, A_2O. While there are other methods that use different silver bases (e.g. AgOAc, Ag_2CO_3), Lin's A_2O method has been shown to be more efficient than those involving other salts, requiring shorter times for similar reactions, which has been attributed to the higher basicity of A_2O.[65,67]

Theoretical studies involving Density Functional Theory (DFT) calculations by the Lledós group have been used to provide mechanistic insight as to why this is the case.[67] Basing their studies on the reaction between Ag_2O and 1,3-dimethylimidazolium iodide in DCM, researchers proposed four possible mechanisms and determined which route was thermodynamically favored from the results of the DFT calculations. They concluded that the mechanism was a combination of two different routes: the sequential monomer pathway and the sequential dimer pathway (**Schemes 3** and **4**). The overall reaction is a thermodynamically driven process (ΔG_{rxn} = -72.9 kcal/mol) involving two imidazolium salts and Ag_2O interacting over a series of very low barrier steps (**Figures 7 and 8**).[67]

The first stage follows the sequential dimer pathway wherein the first NHC salt undergoes a barrierless and exergonic deprotonation by Ag_2O (ΔG = -38.9 kcal/mol) followed by a low barrier exergonic metalation (ΔG = -35.0 kcal/mol) (**Scheme 3**; **Figure 7**).[67] The reaction is driven forward first by the relative acid-base strength of the imidazolium proton and Ag_2O, then by the stabilization of the carbene following the formation of the Ag-C bond. Throughout the process, the second NHC stabilizes both the intermediates (**A** and **C**) and the transition state (**B**) by hydrogen bonding to silver oxide's oxygen, making the reaction even more thermodynamically favorable. This results in approximately a 10 kcal/mol difference between the energy levels of the

25

intermediates and transition states of sequential dimer and sequential monomer pathways during the first deprotonation and metalation steps.[67]
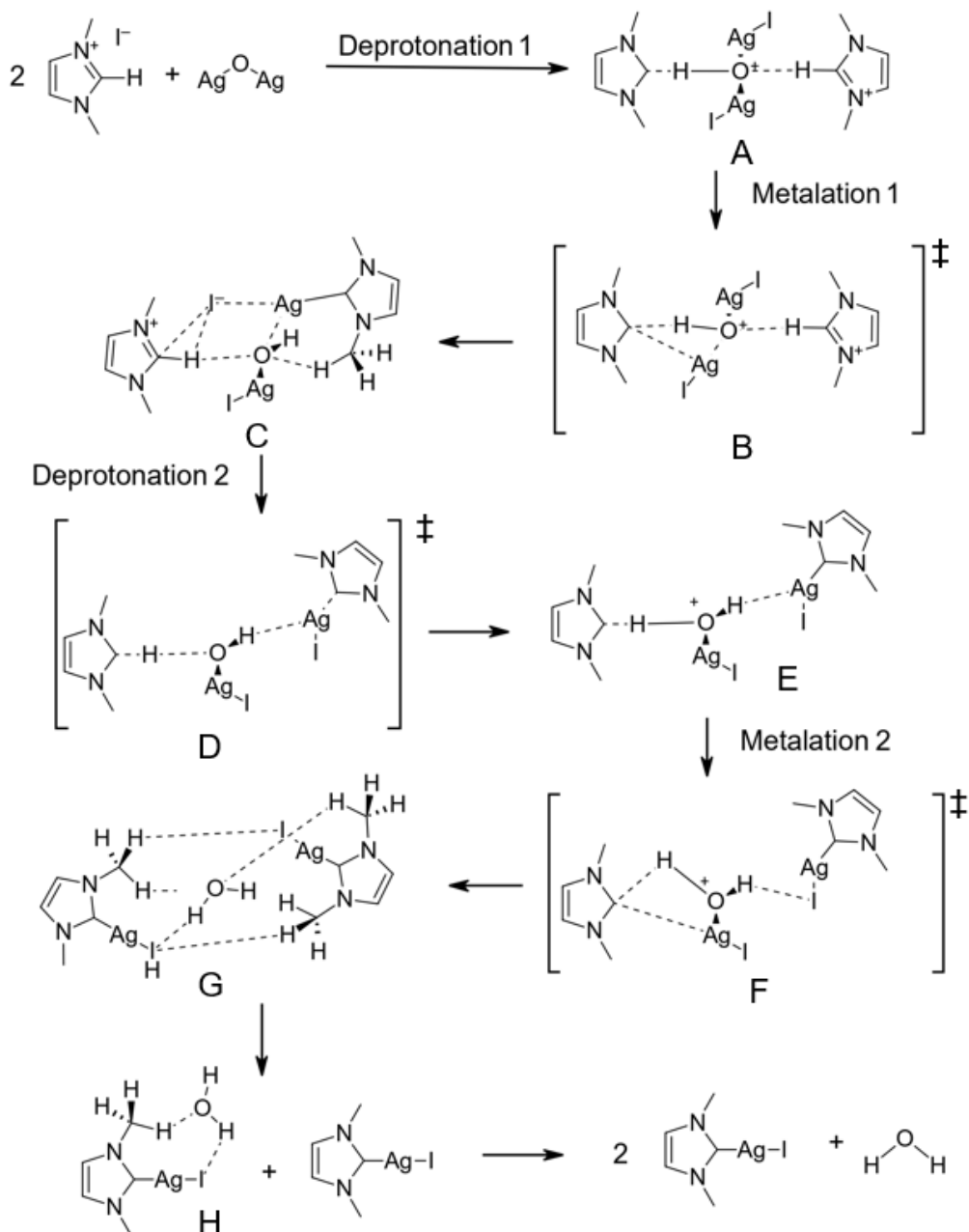
Scheme 3. Ag(I)-NHC formation via the sequential dimer mechanism.[67]
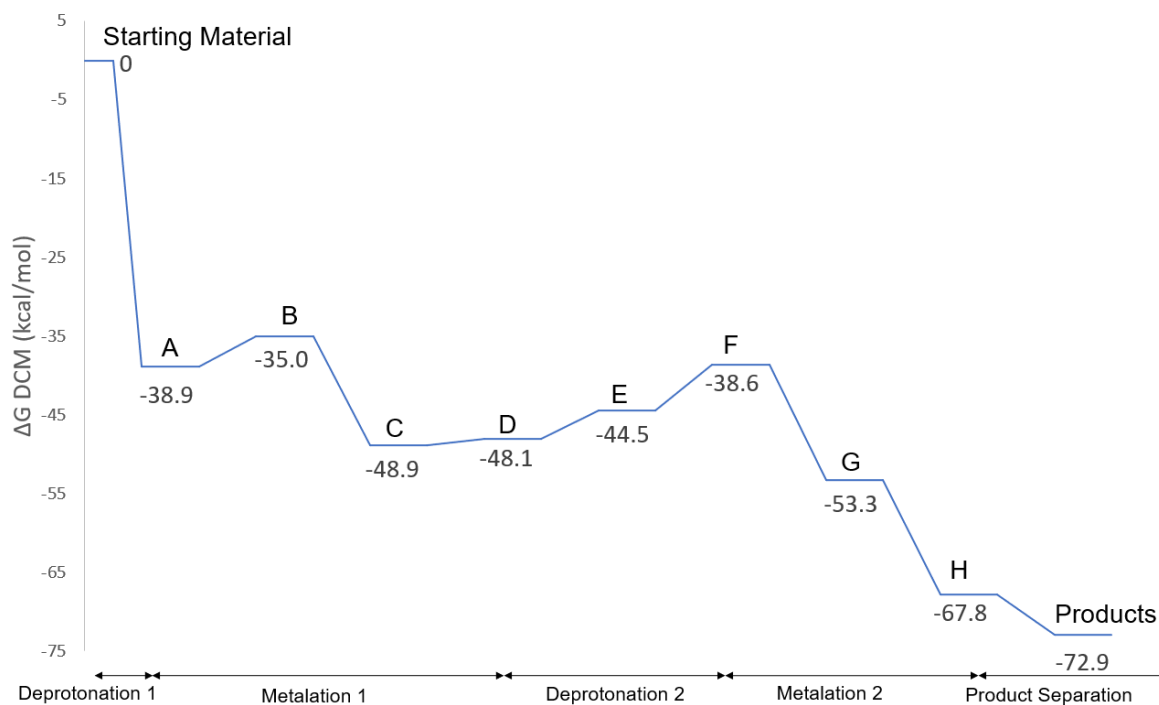
Figure 7. Gibbs free energy profile of the sequential dimer pathway in DCM.[67]

After, the synthesized Ag(I)-NHC complex dissociates from the second NHC salt (Intermediate **C**), forming Intermediate **M** (ΔG = -59.6 kcal/mol) (**Schemes 3** and **4**). Once that occurs, the second NHC undergoes the deprotonation-metalation that occurs in the sequential monomer pathway (**Scheme 4**; **Figure 8**). The second deprotonation is slightly endergonic (ΔG = -58.1 kcal/mol) as the second imidazolium reacts with AgOH, which is a weaker base than Ag_2O. While the second deprotonation has a slightly higher energy barrier and is less exergonic than the first one, the carbene stabilization is enough to drive the reaction forward.[67]
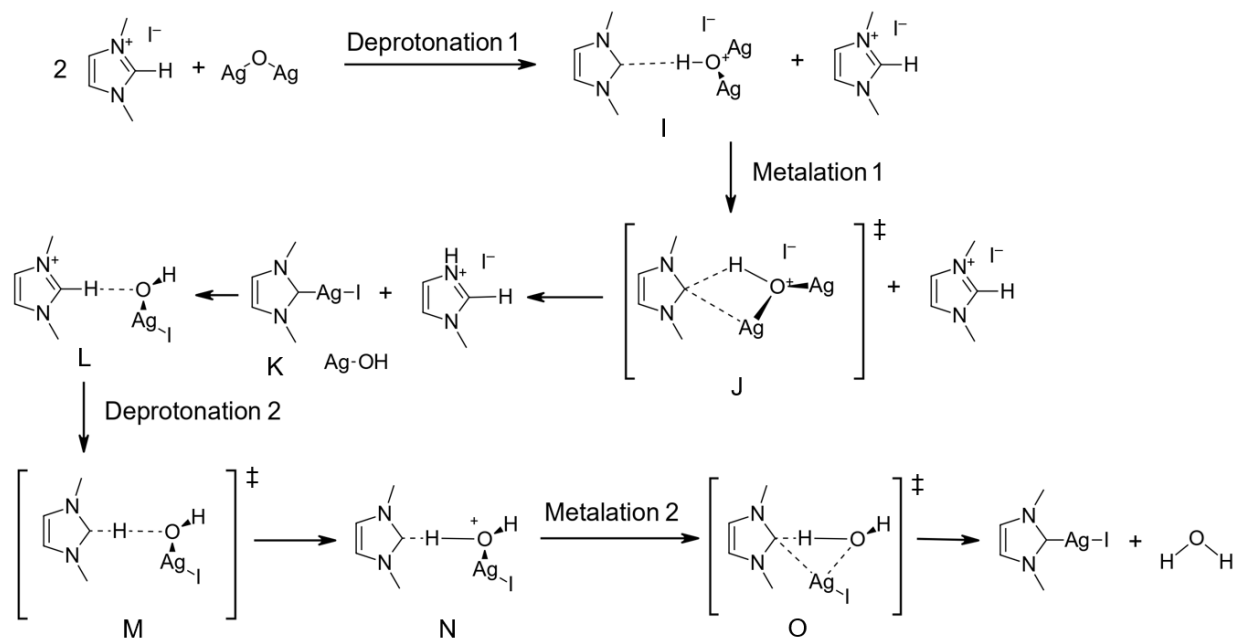
Scheme 4. Ag(I)-NHC formation via the sequential monomer mechanism.[67]
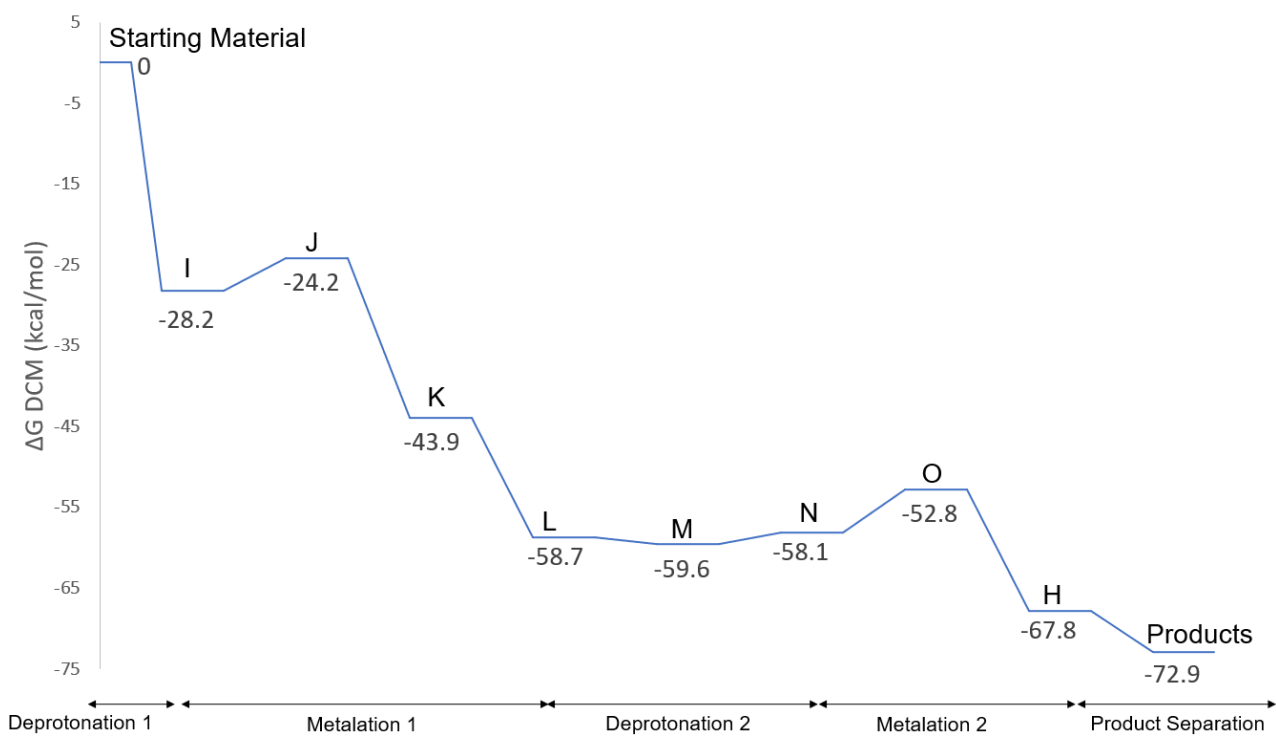
Figure 8. Gibbs free energy profile of the sequential monomer pathway in DCM.[67]

There are several mechanistic reasons that could result in lower yield. Since DCM is a coordinating solvent and has been shown to form complexes with silver, it is possible that it could chelate to Ag_2O, thus reducing its basicity.[67,68] However, the Lledós group concluded that the deprotonation of the imidazolium salt is significantly more favored, and that solvent coordination would not substantially impede the reaction.[67] Another issue could be the structure of the NHC salt as functional groups that decrease the acidity of the imidazolium H have been shown to have reduced reactivity toward Ag_2O and other silver bases.[65] Likewise, significant steric bulk around imidazolium H can also prevent deprotonation in which case reactions involving sterically hindered NHCs tend to require refluxing.[65] The Vasam group's protocol for **1** and **2** did not require refluxing and instead ran at room temperature for 18 hr.[57] Of the remaining three compounds, only **3** and **5** were refluxed. While **5** did have the highest yield, the protocol for **4** did not involve refluxing and resulted in a yield that exceeded the literature yield.[60] A search of the literature shows that both **1** and **2** can be made either at room temperature or with a refluxing step.[60,61,69,70] As such, it seems unlikely that the lack of the refluxing step can account for the discrepancy in yields. Numerous reports have shown that the halide counterion, solvent, and silver: NHC salt ratio can influence the solid-state structure of the resulting Ag(I)-NHCs (**Figure 9**).[66] However, in general, *N,N'*-diaryl substituted imidazolium salts tend to only produce Type 2 complexes when reacting with Ag_2O in DCM.[66]
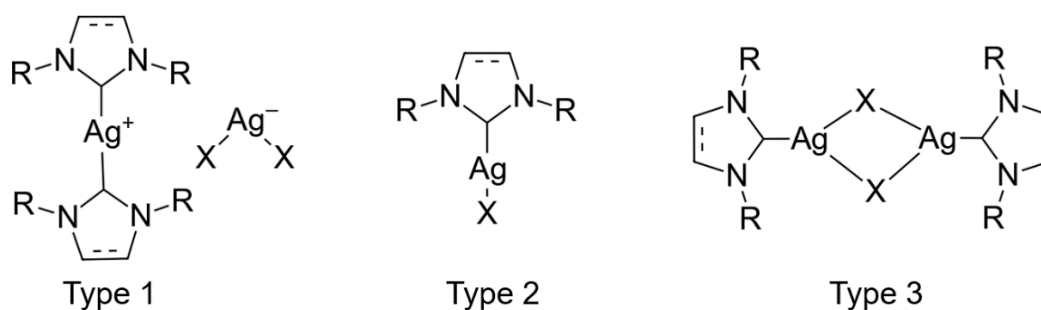
Figure 9. Possible Ag(I)-NHC solid state structures.[66]

However, the most likely reason for the yield discrepancy is the loss of product during the recrystallization process. Complexes **4** and **5** have the highest yields of the five complexes and had different recrystallization or purification protocols from the others. Complex **4** was cooled to 0°C before a slow addition of heptane, resulting in the formation of the crude Ag(I)-NHC that was washed with pentane and dried under vacuum.[60] Meanwhile, **5** was precipitated out of solution via

the addition of pentane and was subsequently washed with more pentane and dried under vacuum.[60] The first three complexes followed a similar recrystallization process. All were concentrated *in vacuo*, redissolved in either THF (**1** and **2**) or DCM (**3**), and had aliquots of nonpolar solvent (hexanes for **1** and **2**, pentane for **3**) added over the course of several days and weeks during which the crystallization solutions were stored in a 0°C freezer. For complexes **1-3**, it is likely that there was remaining product in the mother liquor that was not recovered, thus explaining the low yields. One possible remedy is to optimize the recrystallization protocol by either going slower and adding smaller aliquots of the nonpolar solvent or by utilizing different solvent pairs.

Future Directions

Two more Ag(I)-NHC complexes, **6** and **7**, were originally proposed, but were unable to be successfully synthesized due to time constraints as generating sufficient amounts of complexes **1-5** for the antibacterial studies was prioritized. Upon successful completion of the syntheses, all complexes will be given to the Santiago lab to be screened against *S. mutans*. The results generated from the Santiago lab will inform our choice of structural features for the next series of compounds.

Regarding **6** and **7**, both complexes have increased steric bulk compared to the baseline, **1**, due to the addition of an aromatic benzene group (i.e. BMes) directly to the backbone (**6**) or the replacement of the central imidazoline with a 6-membered diazinane (**7**). Complexes **6** and **7** follow a different synthetic route than the previous five complexes (**Schemes 5** and **6**). Both use a Buchwald-Hartwig amination, a type of C-N cross-coupling reaction, to generate the starting diamine (**11** and **12**). This is followed by a ring-closing reaction to generate the imidazolium (**18**) and pyrimidinium (**19**) salts required for their respective silver coordination reactions.[71-73]
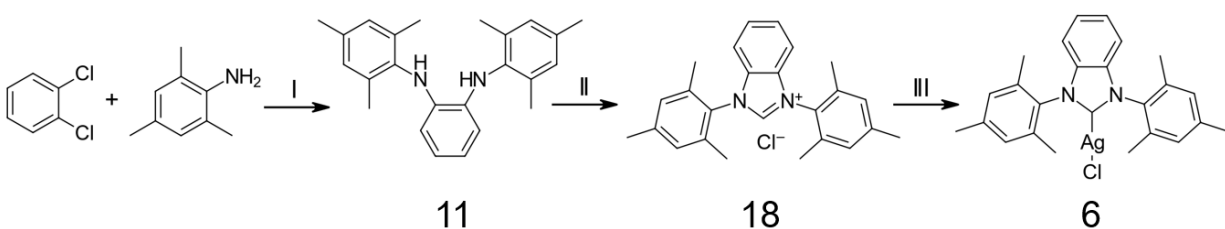
Scheme 5. Synthesis of **6, 11,** and **18**. I) Pd$_2$(dba)$_3$, P(t-Bu)$_3$, NaOt-Bu, 115°, 15 hr, toluene; II) triethyl orthoformate, TMSCl, 145°C, 1.25 hr; III) AgNO$_3$, K$_2$CO$_3$, DCM, RT, 2 hr.[71,72]
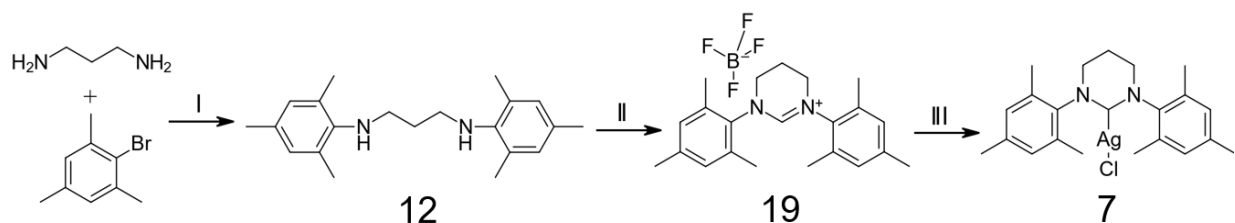
Scheme 6. Synthesis of **7, 12,** and **19**. I) Pd$_2$(dba)$_3$; (rac)-BINAP; NaOt-Bu, 140°, 70 hr, toluene; II) NH$_4$BF$_4$, triethyl orthoformate, 135°C, 17 hr; III) Ag$_2$O; NMe$_4$Cl; DCM.[73]

To date, only the synthesis of **11** has been attempted. A different catalyst, Pd$_2$(dba)$_3$, was used instead of the original, Pd(dba)$_2$, as previous studies indicated no substantial differences in yields between the two catalysts when used in other C-N cross coupling reactions.[71,74] During the first attempt at synthesizing **11**, isolation and work-up generated a pale grey solid which matched the reported appearance.[71] However, the solid failed to dissolve in the reported NMR solvent, CDCl$_3$, as well as CD$_2$Cl$_2$ even after sonication. Further exploration of the literature has found that while the reported appearance of **11** varies widely, the compound is soluble in CDCl$_3$, thus indicating **11** was not successfully made.[75,76] During the second attempt, the amounts of the reagents were kept the same and a 250 mL Schlenk flask was used rather than a pressure tube to ensure that there was sufficient headspace for the reaction to properly reflux. Additionally, the reaction refluxed for 68.25 hr rather than 15 hr and more stringent standards regarding glovebox O$_2$ levels were employed due to Buchwald-Hartwig amination's sensitivity to air.[77] At the end of the second attempt's reflux, the solution had turned dark brown/black whereas during the first attempt, the solution only turned light brown. Isolation and work-up yielded another pale grey solid, but with a higher yield when compared to the first attempt (0.28 g vs 0.09 g). Unfortunately, the previous NMR solvent solubility issues persisted, indicating that **11** was not made.

To understand why the product had failed to form, ^{1}H NMR was used to monitor the coupling of 2,4,6-trimethylaniline to 1,2-dicholormethane in benzene-d$_6$. Over the course of 308.75 hr, the reaction temperature was gradually raised from 40°C to 130°C with ^{1}H NMRs taken of the sample at various time points. Spectral analysis indicated that a reaction did occur as the original peaks began either shifting or disappearing and new peaks began forming after 40 hrs. Based on spectral analysis, the reaction appeared to mostly be complete at 140 hr. While peaks continued to decrease in size or disappear up until the last measurement, there is a chance that that

could be attributed to the decomposition of the synthesized compound. Based on the results of the complexation studies, the ^{1}H NMR monitoring experiment will be repeated using toluene-d$_6$ to determine if the cross-coupling occurred since toluene is the solvent used in the Berke protocol.

Given the spectral data and the fact that products were isolated, it possible that the Buchwald-Hartwig amination did not go to completion, resulting in only the formation of a monochloroaniline rather than the desired diamine. The monochloroaniline product could easily be identified via mass spectroscopy due to characteristic M+ and M+2 molecular ion peaks in a 3:1 ratio. The Diver group had previously developed a similar protocol for synthesizing various benzimidazolium salts, using 1,2-dibromobenzene as the coupling partner, rather than 1,2-dichlorobenzene.[78] Rather than synthesizing the diamine using only one amination like the Berke group, the Diver group set up two subsequent cross-couplings.[71,78] The first coupling yielded a monobromoaniline which was then isolated and purified before being used as the coupling partner in the next Buchwad-Hartwig reaction amination. The reaction conditions reported by the Diver group for the synthesis of the monoaminated products were similar enough to the conditions reported by the Berke group for the diaminated product. In general, the Diver reactions involved lower temperatures, generally ran for longer times, and used a different bulky phosphine (BINAP).[71,78] It is possible that Diver's tandem Buchwald-Amination process could be modified for the Berke protocol to successfully yield **11**.

If subsequent attempts at synthesizing **11** fail, the next step is to alter the reaction conditions. There is some latitude regarding what can go into the Buchwald-Hartwig reaction mixture, as there are numerous reported conditions for C-N cross couplings.[80] In total, there are seven alterable variables that can impact the reaction: the starting materials, the catalyst, the base, the ligands, the solvent, the temperature, and the length of the reaction.[79-82] As such, multiple small-scale Buchwald-Hartwig aminations with varying reaction conditions will be run (**Table 1**). For all reactions, the ligand [P(t-Bu)$_3$], the solvent (toluene), temperature (110°C), and length (24 hr) will remain the same. The most successful reaction from that series will then be scaled up to synthesize **11**. If all those reactions fail to yield **11**, a different protocol will be attempted.

Table 1. Buchwald-Hartwig amination reaction matrix.

Attempt	Catalyst	Base	Ligand	Solvent	Temp (°C)	Length	Yield
1	$Pd_2(dba)_3$	NaOt-Bu	P(t-Bu)$_3$	Toluene	90°C	15 hr	0%
2	$Pd_2(dba)_3$	NaOt-Bu	P(t-Bu)$_3$	Toluene	110°C	69.75 hr	0%
3	$Pd_2(dba)_3$	Cs_2CO_3	P(t-Bu)$_3$	Toluene	110°C	24 hr	TBD
4	$Pd(OAc)_2$	NaOt-Bu	P(t-Bu)$_3$	Toluene	110°C	24 hr	TBD
5	$Pd(OAc)_2$	Cs_2CO_3	P(t-Bu)$_3$	Toluene	110°C	24 hr	TBD

Conclusion

To assess the influence of NHC sterics and electronics on bioactivity against *S. mutans*, a series of Ag(I)-NHC complexes (**1-5**) and their precursors were synthesized with low to moderate yields. Challenges arose during the syntheses of imidazolium chlorides **14** and **15** and complex **3**, requiring multiple attempts to synthesize. For future attempts at synthesizing these compounds, the amount of the catalytic reagents should be increased, and the isolation and recrystallization protocols should be optimized in order to improve overall yields. Future work should prioritize completing the syntheses of [(BMes)AgCl] (**6**) and [(6-Mes)AgCl] (**7**) and generating enough of all the ligands and complexes for the antibacterial assays. After which, all synthesized compounds will be given to the Santiago lab (Rollins Dept. of Biology) where they will be screened against *S. mutans* to assess their antibacterial activity. The data that results from these studies will inform future structural choices for the next series of compounds.

Experimental Methods

General Considerations

All complexation and coupling reactions were done under nitrogen atmosphere in an Inert Lab 2GB Glovebox System (Innovative Technology) or on a Schlenk line. NMR spectra were obtained on a JEOL 300 MHz spectrometer and analyzed using Mnova (v10.0.2). Deuterated solvents were purchased from Cambridge Isotope Laboratories and referenced to the following chemical shifts: CDCl$_3$ (^{1}H: δ7.26; ^{13}C: 77.16), C$_6$D$_6$ (δ7.16), CD$_3$CN (δ1.94), and CD$_2$Cl$_2$ (δ5.32). The DCM, THF, hexanes, pentane, heptane, formic acid, methanol, 2,3-butanedione, paraformaldehyde, chloroform, acetonitrile, sodium bicarbonate, magnesium sulfate, and 1,2-dichlorobenzene were purchased from Sigma Aldrich. The Ag$_2$O, 1,3-bis(2,4,6-trimethylphenyl)imidazolinium chloride, 1,3-bis-(2,6-diisopropylphenyl)imidazolinium chloride, Pd$_2$(dba)$_3$, and P(tBu)$_3$ (10% in hexanes) were purchased from Strem. The glyoxal (40 wt% in H$_2$O) and 2,6-diisopropylaniline were purchased from Alfa Aesar. The Celite was purchased from EMD Millipore. The 2,4,6-trimethylaniline was purchased from Bean Town Chemical. The diethyl ether was purchased from Pharmco. The ethyl acetate was purchased from both Sigma Aldrich and VWR. The 4M HCl in dioxane and sodium t-butoxide were purchased from Oakwood Chemicals.

Syntheses of Ag(I)-NHCs

*Synthesis of [1,3-bis(2,4,6-trimethylphenyl)-imidazol-2-ylidene]silver(I) chloride (**1**)*

Adapted from Vasam, C. S. et al. Imidazolium chloride `**13** (0.467 mmol; 0.189 g) was dissolved in DCM (10 mL). Ag$_2$O (0.2784 mmol; 0.0651 g) was added and the solution stirred at RT for 52 hr. The resulting solution was filtered through Celite and removed from the glovebox. The solution was concentrated *in vacuo* and the resulting solid dissolved in minimal THF. Recrystallization with hexanes at 0°C and vacuum filtration yielded [1,3-bis(2,4,6-trimethylphenyl)-imidazol-2-ylidene]silver(I) chloride (0.069 g; 41%) as a beige, lustrous powder. ^{1}H NMR (300 MHz, CDCl$_3$) δ 7.13 (d, J = 1.8 Hz, 2H), 6.99 (s, 4H), 2.35 (s, 6H), 2.07 (s, 12H).[57]

*Synthesis of [1,3-bis(2,6-diisopropylphenyl)-imidazol-2-ylidene]silver(I) chloride (**2**)*

Adapted from Vasam, C. S. et al. Imidazolium chloride **14** (0.294 mmol; 0.125 g) was dissolved in DCM (2 mL). Ag$_2$O (0.147 mmol; 0.0344 g) was added and the solution stirred at RT for 90.5 hr. The resulting solution was removed from the glovebox and filtered through Celite. The solution

was concentrated *in vacuo* and the resulting solid dissolved in minimal THF. Recrystallization with hexanes at 0°C and vacuum filtration yielded of [1,3-bis[2,6-diisopropylphenyl)]imidazol-2-ylidene]silver(I) chloride (0.0346 g; 22%) as a white powder. ^{1}H NMR (300 MHz, CDCl$_3$) δ 7.53-7.47 (t, J = 9.0 Hz, 2H), 7.31-7.26 (m, J = 7.5 Hz, 4H), 7.21 (s, 2H), 2.58-2.49 (sept, J = 6.75 Hz, 4H), 1.29-1.21 (dd, J = 16.5, 7.5 Hz, 24H).[57]

Synthesis of [(1,3-bis(2,4,6-trimethylphenyl)-4,5-dimethyl-imidazol-2-ylidene]silver chloride (3)
Imidazolium chloride **15** (0.1049 mmol; 0.0387 g) was dissolved in DCM (10 mL). Ag$_2$O (0.1363 mmol; 0.0316 g) was added and the solution stirred at approximately 40°C for 94.5 hr. The resulting solution was removed from the glovebox and filtered through Celite. The solution was concentrated *in vacuo* and the resulting solid dissolved in minimal DCM. Recrystallization with pentane at 0°C and vacuum filtration yielded [(1,3-bis(2,4,6-trimethylphenyl)-4,5-dimethyl-imidazol-2-ylidene]silver chloride (0.0231 g; 46%) as a beige, sparkly powder. ^{1}H NMR (300 MHz, CDCl$_3$) δ 6.98 (s, 4H), 2.34 (s, 6H), 2.00 (s, 12H), 1.90 (s, 6H).

Synthesis of [1,3-bis(2,4,6-trimethylphenyl)imidazolidin-2-ylidene]silver(I) chloride (4)
Adapted from Nolan, S. P. et al. The salt, 1,3-bis(2,4,6-trimethylphenyl)imidazolinium chloride (**16**) (0.333 mmol; 0.114 g) was dissolved in DCM (10 mL). Ag$_2$O (0.383 mmol; 0.0895 g) was added and the solution was refluxed for 5 hr, stirred at RT for 18.5 hr, and refluxed again for 7 hr. The resulting solution stirred at RT for 4 days before being removed from the glovebox and filtered through Celite. The solution was cooled to 0°C and recrystallized with heptane. Vacuum filtration and washing with pentane (10 mL) yielded of [1,3-bis(2,4,6-trimethylphenyl)imidazolidin-2-ylidene]silver(I) chloride (0.115 g; 77%) as a sand brown, flaky solid. ^{1}H NMR (300 MHz, CDCl$_3$) δ 6.95 (s, 4H), 4.00 (s, 4H), 2.29 (s, 18H).[60]

Synthesis of [1,3-bis[2,6-(diisopropylphenyl)]imidazolidin-2-ylidene]silver(I) chloride (5)
Adapted from Nolan, S. P. et al. The salt, 1,3-bis-(2,6-diisopropylphenyl)imidazolinium chloride (**17**) (0.28 mmol; 0.120 g) was dissolved in DCM (10 mL). Ag$_2$O (0.173 mmol; 0.0402 g) was added and the solution stirred at RT for 68.5 hr. The resulting solution was removed from the glovebox and filtered through Celite. The addition of pentane (30 mL) generated a precipitate that was washed with more pentane (3 x 10 mL). Vacuum filtration and drying under vacuum yielded

[1,3-bis[2,6-(diisopropylphenyl)]imidazolidin-2-ylidene]silver(I) chloride (0.0559 g; 37%) as a cream powder. ^{1}H NMR (301 MHz, CDCl[3]) δ 7.44-7.39 (t, $J = 7.5$ Hz, 2H), 7.26-7.23 (cmplx, 4H), 4.07 (s, 4H), 3.12-2.98 (sept, $J = 7.1$ Hz, 4H), 1.36-1.33 (dd, $J = 1.62$ Hz, 24H).[60]

Syntheses of Diazabutadiene Precursors

Synthesis of N,N'-bis(2,4,6-trimethylphenyl)-1,4-diazabutadiene (8)

Adapted from Nolan and Bantreil. Methanol (100 mL) was used to dissolve 2,4,6-trimethylaniline (178.36 mmol; 25 mL). The dark blue solution stirred for 5 minutes before glyoxal (89.19 mmol; 10.2 mL) was added, followed by formic acid (2.42 mmol %). The solution stirred at RT for 23 hr. Vacuum filtration and washing with methanol (3 x 100 mL) yielded *N,N'*-bis(2,4,6-trimethylphenyl)-1,4-diazabutadiene (18.43 g, 71%) as a neon yellow powder. ^{1}H NMR (300 MHz, CDCl[3]) δ 8.10 (s, 2H), 6.91 (s, 1H), 2.29 (s, 6H), 2.16 (s, 12H).[55]

Synthesis of N,N'-bis(2,6-diisopropylphenyl)-1,4-diazabutadiene (9)

Adapted from Nolan and Bantreil. Methanol (8 mL) was used to dissolved 2,6-diisopropylaniline (15.92 mmol; 3 mL). The red solution stirred for 5 minutes before glyoxal (7.97 mmol; 0.9 mL) was added, followed by formic acid (22.7 mmol %). The solution stirred at RT for 21 hr. Vacuum filtration and washing with methanol (3 x 15 mL) yielded *N,N'*-bis(2,6-diisopropylphenyl)-1,4-diazabutadiene (1.92 g, 64%) as a neon yellow powder. ^{1}H NMR (300 MHz, CDCl[3]) δ 8.10 (s, 2H), 7.22-7.16 (m, $J = 4.5$ Hz, 6H), 3.01-2.87 (sept, $J = 6.8$ Hz, 4H), 1.21 (d, $J = 6.9$ Hz, 24H).[55]

Synthesis of N,N'-bis(2,4,6-trimethylphenyl)butane-2,3-diimine (10)

Adapted from Lamaty, Métro, Bantreil, et al. Methanol (240 mL) was used to dissolved 2,4,6-trimethylaniline (237.2 2 mmol; 33 mL). The dark blue solution was cooled to 0°C before 2,3-butanedione (118.6 mmol; 10.3 mL) was added, followed by formic acid (9.7 mmol %). The solution stirred at RT for 48 hr. Vacuum filtration and washing with methanol (2 x 100 mL) and diethyl ether (2 x 100 mL) yielded *N,N'*-bis(2,4,6-trimethylphenyl)butane-2,3-diimine (21.78 g, 57%) as a neon yellow powder. ^{1}H NMR (300 MHz, CDCl[3]) δ 6.89 (s, 4H), 2.29 (s, 6H), 2.03 (s 6H), 2.00 (s, 12H).[58]

Syntheses of Imidazolium Chlorides

Synthesis of 1,3-bis-(2,4,6-trimethylphenyl)imidazolium chloride (13)

Adapted from Nolan, S. P. and Bantreil, X. Compound **8** (17.10 mmol; 5 g) was dissolved in ethyl acetate (35 mL) while paraformaldehyde (18.59 mmol; 0.558 g) was dissolved in 4 M HCl in dioxane (25.65 mmol; 6.41 mL). The paraformaldehyde-HCl solution was added dropwise to the ethyl acetate solution. After gently heating for 1 hr, the reaction mixture stirred at RT for 17 hr. Vacuum filtration, washing with ethyl acetate (3 x 50 mL), and drying under vacuum yielded 1,3-bis-(2,4,6-trimethylphenyl)imidazolium chloride (5.247 g, 90%) as an off-white powder. ^{1}H NMR (300 MHz, CDCl$_3$) δ 10.91 (s, 1H), 7.61 (s, 2H), 7.01 (s, 4H), 2.33 (s, 6H), 2.17 (s, 12 H).[55]

Synthesis of 1,3-bis-(2,6-diisopropylphenyl)imidazolinium chloride (14)

Adapted from Jones, W. et al. Compound **9** (13.27 mmol; 5 g) was dissolved in ethyl acetate (30 mL) while paraformaldehyde (14.59 mmol; 0.4381 g) was dissolved in 4 M HCl in dioxane (19.90 mmol; 5 mL). The paraformaldehyde-HCl solution was added dropwise to the ethyl acetate solution and the reaction mixture stirred at RT for 20 hr. The precipitate was vacuum filtered and washed with ethyl acetate before being dissolved in chloroform. Concentrating *in vacuo* and drying under vacuum yielded 1,3-bis-(2,6-diisopropylphenyl)imidazolinium chloride (3.94 g, 70%) as a light brown powder. ^{1}H NMR (300 MHz, CDCl$_3$) δ 10.05 (s, 1H), 8.15 (s, 2H), 7.57 (t, J = 7.9 Hz, 2H), 7.34 (d, J = 7.8 Hz, 4H), 2.46-2.43 (m, J = 4.5 Hz, 4H), 1.30-1.23 (dd, J = 15.0, 6.0 Hz, 24H).[56]

Synthesis of [1,3-bis(2,4,6-trimethylphenyl)-4,5-methyl]imidazolium chloride (15)

Adapted from Louie, J. et al. and Lamaty, F. et al. Compound **10** (23.3 mmol; 9.44 g) was dissolved in ethyl acetate (400 mL) cooled to 0°C. Paraformaldehyde (30.3 mmol; 1.02 g) and 4 M HCl in dioxane (37.3 mmol; 9.3 mL) were dissolved in ethyl acetate (100 mL). After being placed in an ice bath for 10 min, the paraformaldehyde-HCl solution was added to the **10** solution and the mixture stirred at RT for 19.75 hr. The resulting terracotta precipitate was vacuum filtered and washed with diethyl ether (2.5 L). Precipitate was stored in diethyl ether (100 mL) and stirred for 18 days. Light brown solid was vacuum filtered and dissolved in methanol (50 mL) and acetonitrile (50 mL). The solution was stirred with NaHCO$_3$ for 30 min before being filtered and concentrated *in vacuo.* The resulting oily residue was triturated with pentane (8 x 15 mL), yielding both brown

granules and solids. Granules were discarded while the solids were dried via rotary evaporation. The resulting light brown powder was dissolved in saturated $NaHCO_3$ and washed with ethyl acetate (4 x 100 mL). Extraction with DCM (3 x 100 mL), drying with $MgSO_4$, and concentration *in vacuo* yielded [1,3-bis(2,4,6-trimethylphenyl)-4,5-methyl]imidazolium chloride (1.3591 g; 16%) as a beige flaky powder. ^{1}H NMR (300 MHz, $CDCl_3$) δ 10.82 (s, 1H), 7.03 (s, 4H), 2.34 (s, 6H), 2.12 (s, 12H), 2.06 (s, 6H). ^{1}H NMR (300 MHz, CD_3CN) δ 8.90 (s, 1H), 7.15 (s, 4H), 2.35 (s, 6H), 2.04 (s, 12H), 2.00 (cmplx, 6H).[58,59]

^{1}H NMR Reaction Monitoring Studies

Monitoring the Complexation of 15 to Silver(I)

Imidazolium chloride **15** (0.040657 mmol; 0.015 g) and Ag_2O (0.05285 mmol; 0.01225 g) were dissolved CD_2Cl_2 (~0.5 mL) in a J. Young tube. The tube was taken out of the glovebox and an initial NMR was taken before being placed in a 40°C oil bath for 14.75 hours after which another NMR was taken. The oil bath temperature was raised to 50°C before placing the J. Young back in. NMRs were taken at 24 hr intervals for the next three days.

Monitoring the Cross-Coupling of 2,4,6-trimethylaniline to 1,2-dicholormethane in benzene-d_6

Adapted from Berke, H. et al. Under nitrogen, a round bottom flask was charged with $Pd_2(dba)_3$ (0.01 mmol; 0.00915 g), followed by $P(tBu)_3$ (0.022 mmol; 0.07 mL) and C_6D_6 (5 mL) and stirred at RT for 10 min. The flask was then charged with 1,2-dichlorobenzene (1.43 mmol; 0.161 mL), 2,4,6-trimethylaniline (4.08 mmol; 0.573 mL), NaOtBu (4.09 mmol, 0.393 g), and additional C_6D_6 (5 mL). An aliquot (~0.5 mL) was taken and placed in a J. Young tube. The tube was taken out of the glovebox and an initial NMR was taken before being placed in a 40°C oil bath for 15 hr after which another NMR was taken. The oil bath temperature was raised to 70°C before placing the J. Young back in. An NMR was taken 25 hr later after which the bath temperature was raised to 100°C and then returned to RT. An additional NMR was taken at t=140.75 hr before the bath temperature was raised to 115°C. NMRs were taken 24 and 43 hrs later. The oil bath temperature was raised to 130°C before and an NMR was taken 24 hr later. J. Young was cooled to RT and a final NMR was taken at t=308.75 hr.[72]

References

1. Orvig, C.; Abrams, M. J. Medicinal Inorganic Chemistry: Introduction. *Chem. Rev.* **1999**, *99* (9), 2202–2203.

2. Mjos, K. D.; Orvig, C. Metallodrugs in Medicinal Inorganic Chemistry. *Chemical Reviews*. **2014,** *114* (8), 4540-4563

3. Valent, P.; Groner, B.; Schumacher, U.; Superti-Furga, G.; Busslinger, M.; Kralovics, R.; Zielinski, C.; Penninger, J. M.; Kerjaschki, D.; Stingl, G.; Smolen, J. S.; Valenta, R.; Lassmann, H.; Kovar, H.; Jäger, U.; Kornek, G.; Müller, M.; Sörgel, F. Paul Ehrlich (1854-1915) and His Contributions to the Foundation and Birth of Translational Medicine. *J. Innate Immun.* **2016**, *8* (2), 111–120.

4. Medici, S.; Peana, M.; Nurchi, V. M.; Zoroddu, M. A. Medical Uses of Silver: History, Myths, and Scientific Evidence. *J. Med. Chem.* **2019**, *62* (13), 5923–5943.

5. WHO. *Silver as a Drinking-Water Disinfectant*; 2018.

6. Barillo, D. J.; Marx, D. E. Silver in Medicine: A Brief History BC 335 to Present. *Burns* **2014**, *40* (S1), S3–S8.

7. States, T. U. National Strategy for Combating Antibiotic-Resistant Bacteria. *CDC*. **2014**, 1– 40.

8. Marx, D. E.; Barillo, D. J. Silver in Medicine: The Basic Science. *Burns* **2014**, *40* (S1), S9–S18.

9. Trotter, K. D.; Owojaiye, O.; Meredith, S. P.; Keating, P. E.; Spicer, M. D.; Reglinski, J.; Spickett, C. M. The Interaction of Silver(II) Complexes with Biological Macromolecules and Antioxidants. *BioMetals.* **2019**, *32* (4), 627–640.

10. Chellan, P.; Sadler, P. J. The Elements of Life and Medicines. *Phil. Trans. R. Soc. A* **2015**, *373*.

11. Medici, S.; Peana, M.; Nurchi, V. M.; Lachowicz, J. I.; Crisponi, G.; Zoroddu, M. A. Noble Metals in Medicine: Latest Advances. *Coordination Chemistry Reviews*. Elsevier B.V. February 1, **2015**, 329–350.

12. Zhang, S.; Du, C.; Wang, Z.; Han, X.; Zhang, K.; Liu, L. Reduced Cytotoxicity of Silver Ions to Mammalian Cells at High Concentration Due to the Formation of Silver Chloride. *Toxicol. Vitr.* **2013**, *27* (2), 739–744.

13. Egorova, K. S.; Ananikov, V. P.; Zelinsky, N. D. Toxicity of Metal Compounds: Knowledge and Myths. *Organometallics.* **2017,** *36* (21), 4071-4090

14. Bertrand, G. *8th Int. Conf. Appl. Chem*. **1912**, *28*, 30.

15. Falzone, L.; Salomone, S.; Libra, M. Evolution of Cancer Pharmacological Treatments at the Turn of the Third Millennium. *Front. Pharmacol.* **2018**, *9* (1300).

16. Chen, Y.; Huang, Z.; Xu, J. F.; Sun, Z.; Zhang, X. Cytotoxicity Regulated by Host-Guest Interactions: A Supramolecular Strategy to Realize Controlled Disguise and Exposure. *ACS Appl. Mater. Interfaces* **2016**, *8* (35), 22780–22784.

17. Medici, S.; Peana, M.; Crisponi, G.; Nurchi, V. M.; Lachowicz, J. I.; Remelli, M.; Zoroddu, M. A. Silver Coordination Compounds: A New Horizon in Medicine. *Coordination Chemistry Reviews*. Elsevier B.V. November 15, 2016, 349–359.

18. Wang, H.; Yan, A.; Liu, Z.; Yang, X.; Xu, Z.; Wang, Y.; Wang, R.; Koohi-Moghadam, M.; Hu, L.; Xia, W.; et al. Deciphering Molecular Mechanism of Silver by Integrated Omic Approaches Enables Enhancing Its Antimicrobial Efficacy in E. Coli; *PLoS Biol*. **2019**, *17*(6).

19. Königs, A. M.; Flemming, H. C.; Wingender, J. Nanosilver Induces a Non-Culturable but Metabolically Active State in Pseudomonas Aeruginosa. *Front. Microbiol.* **2015**, *6* (395), 1–11.

20. Wakshlak, R. B. K.; Pedahzur, R.; Avnir, D. Antibacterial Activity of Silver-Killed Bacteria: The "Zombies" Effect. *Sci. Rep.* **2015**, *5*, 1–5.

21. Porto, V.; Borrajo, E.; Buceta, D.; Carneiro, C.; Huseyinova, S.; Domínguez, B.; Borgman, K. J. E.; Lakadamyali, M.; Garcia-Parajo, M. F.; Neissa, J.; García-Caballero, T.; Barone, G.; Blanco, M. C.; Busto, N.; García, B.; Leal, J. M.; Blanco, J.; Rivas, J.; López-Quintela, M. A.; Domínguez, F. Silver Atomic Quantum Clusters of Three Atoms for Cancer Therapy: Targeting Chromatin Compaction to Increase the Therapeutic Index of Chemotherapy. *Adv. Mater.* **2018**, *30* (33).

22. Yu, Y.; Mok, B. Y. L.; Loh, X. J.; Tan, Y. N. Rational Design of Biomolecular Templates for Synthesizing Multifunctional Noble Metal Nanoclusters toward Personalized Theranostic Applications. *Adv. Healthc. Mater.* **2016**, *5* (15), 1844–1859.

23. Shen, M.; Forghani, F.; Kong, X.; Liu, D.; Ye, X.; Chen, S.; Ding, T. Antibacterial Applications of Metal–Organic Frameworks and Their Composites. *Compr. Rev. Food Sci. Food Saf.* **2020**, *19* (4), 1397–1419.

24. Roy, A.; Bulut, O.; Some, S.; Mandal, A. K.; Yilmaz, M. D. Green Synthesis of Silver Nanoparticles: Biomolecule-Nanoparticle Organizations Targeting Antimicrobial Activity. *RSC Advances*. January 18, 2019, 2673–2702.

25. Van Der Tol, J.; Jia, D.; Li, Y.; Chernyy, V.; Bakker, J. M.; Nguyen, M. T.; Lievens, P.; Janssens, E. Structural Assignment of Small Cationic Silver Clusters by Far-Infrared Spectroscopy and DFT Calculations. *Phys. Chem. Chem. Phys.* **2017**, *19* (29), 19360–19368.

26. Miao, C.; Su, T. E. Self-Assembly of Two Ag(I) Metal-Organic Frameworks Based on Tri(Pyridin-4-Yl)Amine: Crystal Structures, Anion-Directed Effect, and Cr2O72− Capture Behaviour. *Inorg. Chem. Commun.* **2020**, *112*, 107733.

27. File:Silver sulfadiazine Structural Formula V1.svg - Wikimedia Commons https://commons.wikimedia.org/wiki/File:Silver_sulfadiazine_Structural_Formula_V1.svg (accessed Feb 3, 2021).

28. Silver Nanoparticle Clinical Trials https://clinicaltrials.gov/ct2/results?term=silver+nanoparticle&Search=Clear&age_v=&gndr=&type=&rslt= (accessed Mar 31, 2021).

29. Silver nanoparticle Phase 4 Clinical Trials. https://clinicaltrials.gov/ct2/results?term=silver+nanoparticle&age_v=&gndr=&type=&rslt=&phase=3&Search=Apply (accessed Mar 31, 2021).

30. Comparison of Central Venous Catheters With Silver Nanoparticles Versus Conventional Catheters (NanoAgCVC) https://clinicaltrials.gov/ct2/show/NCT00337714?term=silver+nanoparticle&phase=3&draw=2&rank=1 (accessed Mar 31, 2021).

31. Assessment of Postoperative Pain After Using Various Intracanal Medication in Patients With Necrotic Pulp https://clinicaltrials.gov/ct2/show/NCT03692286?term=silver+nanoparticle&phase=3&draw=2&rank=2 (accessed Mar 31, 2021).

32. Evaluation of Antimicrobial Efficacy and Adaptability of Bioceramic Sealer Containing Nanoparticles https://clinicaltrials.gov/ct2/show/NCT04481945?term=silver+nanoparticle&phase=3&draw=2&rank=3 (accessed Mar 31, 2021).

33. Preadmission Skin Wipe Use for Surgical Site Infection Prophylaxis in Adult Orthopaedic Surgery Patients https://clinicaltrials.gov/ct2/show/NCT03401749?term=silver+nanoparticle&phase=3&draw=2&rank=4(accessed Mar 31, 2021).

34. In-Vivo Assessment of Silver Biomaterial Nano-Toxicity 32 Ppm https://clinicaltrials.gov/ct2/show/NCT01405794?term=silver+nanoparticle&draw=2&rank=22 (accessed Mar 31, 2021).

35. In Vivo Assessment of Silver Biomaterial Nano-Toxicity https://clinicaltrials.gov/ct2/show/

NCT01243320?term=silver+nanoparticle&draw=2&rank=24 (accessed Mar 31, 2021).

36. Munger, M. A.; Radwanski, P.; Hadlock, G. C.; Stoddard, G.; Shaaban, A.; Falconer, J.; Grainger, D. W.; Deering-Rice, C. E. In Vivo Human Time-Exposure Study of Orally Dosed Commercial Silver Nanoparticles. *Nanomedicine Nanotechnology, Biol. Med.* **2014**, *10* (1), 1–9.

37. Blass, B. *Basic Principles of Drug Discovery and Development*, 1st ed.; Elsevier Inc.: London, UK, **2015**, 227.

38. Gerasimchuk, N.; Gamian, A.; Glover, G.; Szponar, B. Light Insensitive Silver(I) Cyanoximates as Antimicrobial Agents for Indwelling Medical Devices. *Inorg. Chem.* **2010**, *49* (21), 9863–9874.

39. Gerasimchuk, N. Synthesis, Properties, and Applications of Light-Insensitive Silver(I) Cyanoximates. *Eur. J. Inorg. Chem.* **2014**, *2014* (27), 4518–4531.

40. Roymahapatra, G.; M. Mandal, S.; F. Porto, W.; Samanta, T.; Giri, S.; Dinda, J.; L. Franco, O.; K. Chattaraj, P. Pyrazine Functionalized Ag(I) and Au(I)-NHC Complexes Are Potential Antibacterial Agents. *Curr. Med. Chem.* **2012**, *19* (24), 4184–4193.

41. Hopkinson, M. N.; Richter, C.; Schedler, M.; Glorius, F. An Overview of *N*-Heterocyclic Carbenes. *Nature*. **2014**, *510* (7506), 485–496.

42. Housecroft, C. E. *Inorganic Chemistry*, 4th ed.; Pearson Education Limited: Harlow, England, **2012**, 665-716.

43. Huynh, H. V. Electronic Properties of *N*-Heterocyclic Carbenes and Their Experimental Determination. *Chem. Rev.* **2018**, *118* (19), 9457–9492.

44. Kendall, A. J.; Tyler, D. R. The Synthesis of Heteroleptic Phosphines. *Dalt. Trans.* **2015**, *44* (28), 12473–12483.

45. Wilson, D. J. D.; Couchman, S. A.; Dutton, J. L. Are *N*-Heterocyclic Carbenes "Better" Ligands than Phosphines in Main Group Chemistry? A Theoretical Case Study of Ligand-Stabilized E 2 Molecules, L-E-E-L (L = NHC, Phosphine; E = C, Si, Ge, Sn, Pb, N, P, As, Sb, Bi). *Inorg. Chem.* **2012**, *51* (14), 7657–7668.

46. Benhamou, L.; Chardon, E.; Lavigne, G.; Bellemin-Laponnaz, S.; César, V. Synthetic Routes to *N*-Heterocyclic Carbene Precursors. *Chem. Rev.* **2011,** *111* (4), 2705-2733.

47. Oun, R.; Moussa, Y. E.; Wheate , N. J. The Side Effects of Platinum Based Chemotherapy Drugs: A Review for Chemists. *Dalton Transactions*. **2018**, *9*, 6645 6653.

48. Ohmichi, M.; Hayakawa, J.; Tasaka , K.; Kurachi , H.; Murata, Y. Mechanisms of Platinum Drug Resistance. Trends in Pharmacological Sciences. Elsevier Ltd March 1, 2005, 113-116.

49. Johnson, N. A.; Southerland, M. R.; Youngs, W. J. Recent Developments in the Medicinal Applications of Silver-NHC Complexes and Imidazolium Salts. *Molecules* **2017**, *22* (8), 1–20.

50. Eloy, L.; Jarrousse, A.-S.; Teyssot, M.-L.; Gautier, A.; Morel, L.; Jolivalt, C.; Cresteil, T.; Roland, S. Anticancer Activity of Silver-*N*-Heterocyclic Carbene Complexes: Caspase-Independent Induction of Apoptosis via Mitochondrial Apoptosis-Inducing Factor (AIF). *ChemMedChem* **2012**, *7* (5), 805–814.

51. Donlan, R. M.; William Costerton, J. Biofilms: Survival Mechanisms of Clinically Relevant Microorganisms. *Clin. Microbiol. Rev.* **2002**, *15* (2), 167–193.

52. Bryers, J. D. Medical Biofilms. *Biotechnology and Bioengineering*. **2008**, *100* (1), 1–18.

53. Cyphert, E. L.; Von Recum, H. A. Emerging Technologies for Long-Term Antimicrobial Device Coatings: Advantages and Limitations. *Exp. Biol. Med.* **2017**, *242*, 788–798.

54. Metwalli, K. H.; Khan, S. A.; Krom, B. P.; Jabra-Rizk, M. A. Streptococcus Mutans, Candida Albicans, and the Human Mouth: A Sticky Situation. *PLoS Pathog.* **2013**, *9* (10).

55. Bantreil, X.; Nolan, S. P. Synthesis of *N*-Heterocyclic Carbene Ligands and Derived Ruthenium Olefin Metathesis Catalysts. *Nat. Protoc.* **2011**, *6* (1), 69–77.

56. Dibenedetto, T. A.; Parsons, A. M.; Jones, W. D. Markovnikov-Selective Hydroboration of Olefins Catalyzed by a Copper *N*-Heterocyclic Carbene Complex. *Organometallics* **2019**, *38* (17), 3322–3326.

57. Thirukovela, N. S.; Balaboina, R.; Kankala, S.; Vadde, R.; Vasam, C. S. Activation of Nitriles by Silver(I) *N*-Heterocyclic Carbenes: An Efficient on-Water Synthesis of Primary Amides. *Tetrahedron* **2019**, *75* (18), 2637–2641.

58. Beillard, A.; Bantreil, X.; Métro, T. X.; Martinez, J.; Lamaty, F. Mechanochemistry for Facilitated Access to N,N-Diaryl NHC Metal Complexes. *New J. Chem.* **2017**, *41* (3), 1057–1063.

59. Van Ausdall, B. R.; Glass, J. L.; Wiggins, K. M.; Aarif, A. M.; Louie, J. A Systematic Investigation of Factors Influencing the Decarboxylation of Imidazolium Carboxylates. *J. Org. Chem.* **2009**, *74* (20), 7935–7942.

60. De Frémont, P.; Scott, N. M.; Stevens, E. D.; Ramnial, T.; Lightbody, O. C.; Macdonald, C.

L. B.; Clyburne, J. A. C.; Abernethy, C. D.; Nolan, S. P. Synthesis of Well-Defined *N*-Heterocyclic Carbene Silver(I) Complexes. *Organometallics* **2005**, *24* (26), 6301–6309.

61. Ramnial, T.; Abernethy, C. D.; Spicer, M. D.; McKenzie, I. D.; Gay, I. D.; Clyburne, J. A. C. A Monomeric Imidazol-2-Ylidene-Silver(I) Chloride Complex: Synthesis, Structure, and Solid State 109Ag and 13C CP/MAS NMR Characterization. *Inorg. Chem.* **2003**, *42* (5), 1391–1393.

62. Yuan, J.; Wang, X.; Mei, T.; Liu, Y.; Miao, C.; Xie, X. An α-Diimine-Nickel(II) Catalyst Bearing an Electron-Withdrawing Substituent for Olefin Polymerization. *Transit. Met. Chem.* **2011**, *36* (4), 433–439.

63. Darvell, B. W. *Materials Science for Dentistry*, 10th ed. Elsevier Ltd. **2018**.

64. Atwood, J. D.; Jacobs, M. L. *United States Patent Office PARAFORMALDEHYDE DEPOLYMERIZATION SOLVENT MEDIA*; 1965.

65. Garrison, J. C.; Youngs, W. J. Ag(I) *N*-Heterocyclic Carbene Complexes: Synthesis, Structure, and Application. *Chemical Reviews*. **2005**, *105* (11), 3978-4008.

66. Lin, I. J. B.; Vasam, C. S. Preparation and Application of *N*-Heterocyclic Carbene Complexes of Ag(I). *Coordination Chemistry Reviews*. **2007**, *251* (5–6), 642–670.

67. Hayes, J. M.; Viciano, M.; Peris, E.; Ujaque, G.; Lledós, A. Mechanism of Formation of Silver *N*-Heterocyclic Carbenes Using Silver Oxide: A Theoretical Study. *Organometallics* **2007**, *26* (25), 6170–6183.

68. Newbound, T. D.; Colsman, M. R.; Miller, M. M.; Wulfsberg, G. P.; Anderson, O. P.; Strauss, S. H. Dichloromethane Is a Coordinating Solvent. *J. Am. Chem. Soc.* **1989**, *111* (10), 3762–3764.

69. Latendorf, K.; Mechler, M.; Schamne, I.; Mack, D.; Frey, W.; Peters, R. Titanium Salen Complexes with Appended Silver NHC Groups as Nucleophilic Carbene Reservoir for Cooperative Asymmetric Lewis Acid/NHC Catalysis. *European J. Org. Chem.* **2017**, *2017* (28), 4140–4167.

70. Cesari, C.; Conti, S.; Zacchini, S.; Zanotti, V.; Cassani, M. C.; Mazzoni, R. Sterically Driven Synthesis of Ruthenium and Ruthenium-Silver *N*-Heterocyclic Carbene Complexes. *Dalt. Trans.* **2014**, *43* (46), 17240–17243.

71. Grieco, G.; Blacque, O.; Berke, H. A Facile Synthetic Route to Benzimidazolium Salts Bearing Bulky Aromatic N-Substituents. *Beilstein J. Org. Chem.* **2015**, *11*, 1656–1666.

72. Wang, W. Toward the Synthesis of Catalytic Conducting Metallopolymer for Cross- Coupling

Reactions, University of Texas at Austin, 2016.

73. Herrmann, W. A.; Schneider, S. K.; Öfele, K.; Sakamoto, M.; Herdtweck, E. First Silver Complexes of Tetrahydropyrimid-2-Ylidenes. *J. Organomet. Chem.* **2004**, *689* (15), 2441–2449.

74. Cong, M.; Fan, Y.; Raimundo, J. M.; Tang, J.; Peng, L. Pd(Dba)$_2$ vs Pd$_2$(Dba)$_3$: An in-Depth Comparison of Catalytic Reactivity and Mechanism via Mixed-Ligand Promoted C-N and C-S Coupling Reactions. *Org. Lett.* **2014**, *16* (16), 4074–4077.

75. Dickschat, J. V.; Urban, S.; Pape, T.; Glorius, F.; Hahn, F. E. Sterically Demanding and Chiral N,N′-Disubstituted *N*-Heterocyclic Germylenes and Stannylenes. *Dalt. Trans.* **2010**, *39* (48), 11519–11521.

76. Wang, Z.; Chen, X.; Xie, H.; Wang, D.; Huang, H.; Deng, G.-J. Synthesis of O-Arylenediamines through Elemental Sulfur-Promoted Aerobic Dehydrogenative Aromatization of Cyclohexanones with Arylamines. *Org. Lett.* **2018**, *20*, 37.

77. Yaseneva, P.; Hodgson, P.; Zakrzewski, J.; Falß, S.; Meadows, R. E.; Lapkin, A. A. Continuous Flow Buchwald-Hartwig Amination of a Pharmaceutical Intermediate. *React. Chem. Eng.* **2016**, *1* (2), 229–238.

78. Rivas, F. M.; Riaz, U.; Giessert, A.; Smulik, J. A.; Diver, S. T. A Versatile Synthesis of Substituted Benzimidazolium Salts by an Amination/Ring Closure Sequence. *Org. Lett.* **2001**, *3* (17), 2673–2675.

79. Ruiz-Castillo, P.; Buchwald, S. L. Applications of Palladium-Catalyzed C-N Cross-Coupling Reactions. *Chemical Reviews*. **2016**, *116* (19), 12564-12649.

80. Beletskaya, I. P.; Cheprakov, A. V. The Complementary Competitors: Palladium and Copper in C-N Cross-Coupling Reactions. *Organometallics*. **2012**, *31* (22), 7753-7808.

81. Kim, S. T.; Kim, S.; Baik, M. H. How Bulky Ligands Control the Chemoselectivity of Pd-Catalyzed: N -Arylation of Ammonia. *Chem. Sci.* **2020**, *11* (4), 1017–1025.

82. Kashani, S. K.; Jessiman, J. E.; Newman, S. G. Exploring Homogeneous Conditions for Mild Buchwald-Hartwig Amination in Batch and Flow. *Org. Process Res. Dev.* **2020**.